tapraid3/zpt-pt/zpt-pt/zpt00810/zpt9037d10z | xppws | S=1 | 5/15/10 | 1:17 | Art: 168070 | Input-KAF

to metastasize to the lung (Saiki, 1997). Western blotting analysis revealed no expression of claudin-4 in B16 cells (Fig. 1A). B16 cells were not sensitive to C-CPE-PSIF (Fig. 2A). We transfected claudin-4 cDNA into B16 cells and established stable CL4-B16 cells (Fig. 1A). The proliferation rate was not affected by exogenously expressed claudin-4 (Fig. 1B). Metastasis has multiple processes, including motility and invasion (Steeg, 2006). To investigate the invasion of CL4-B16 cells, we performed a Boyden chamber migration assay. Cells were seeded onto the cell culture insert of Matrigel-coated membrane with an 8-μm pore size, and the cells that invaded the apical membrane and reached the basal membrane were counted. As shown in Fig. 1C, the invasion activity was increased 17-fold in CL4-B16 cells compared with that in parental B16 cells. Lung metastasis of CL4-B16 cells was observed when intravenously injected into mice; however, the number of lung metastasis colonies of CL4-B16 cells was smaller than that of the parental B16 cells (Fig. 1D). These findings indicate that CL4-B16 cells can be used as a metastasis model of claudin-4-expressing cancer cells. We discuss the elevation of migration activity and lower lung metastasis in CL4-B16 cells under *Discussion*.

Antitumor Activity of C-CPE-PSIF in CL4-B16 Cells. Before in vivo experiments, we investigated the in vitro cytotoxicity of C-CPE-PSIF in CL4-B16 cells. As shown in Fig. 2A, C-CPE-PSIF showed dose-dependent cytotoxicity in CL4-B16 cells, decreasing their viability to 35% at 100 ng/ml. In contrast, parental B16 cells were not sensitive to C-CPE-PSIF even at 1 μg/ml, indicating that C-CPE-PSIF may target claudin-4. Claudin-4 is expressed in the intestines, liver, and kidney (Morita et al., 1999). To determine a safe dose of C-CPE-PSIF, we checked serum biochemical markers of liver (alanine aminotransferase) and kidney (blood urea nitrogen) injury in mice injected with C-CPE-PSIF. After intravenous administration of C-CPE-PSIF (5 μg/kg), the mice showed no signs of injury (data not shown). In the following in vivo experiments, the doses of C-CPE-PSIF were less than or equal to 5 μg/kg. B16 or CL4-B16 cells were intravenously injected into mice, and then C-CPE-PSIF was intravenously administered every 2 days. Two weeks after the tumor cell injection, the number of lung metastasis colonies was counted. As shown in Fig. 2B, C-CPE-PSIF treatment decreased the number of lung metastasis colonies from 39 ± 17 to 10 ± 4 at 5 μg/kg. In contrast, C-CPE-PSIF treatment did not affect the lung metastasis of B16 cells (Fig. 2B). C-CPE-PSIF suppressed the growth of CL4-B16 cells but not B16 cells inoculated into the right flank of mice (Fig. 2C). These data suggest that claudin-4 targeting may be a potent strategy for suppressing tumor metastasis and growth.

Suppression of the Primary Tumors and Metastasis of 4T1 Cells. To clarify the potency of a claudin-4-targeting strategy, we investigated the effect of C-CPE-PSIF on a spontaneous metastasis model. 4T1 cells are murine cancer cells that spontaneously metastasize to the lung after being subcutaneously inoculated (Wong et al., 2002). We investigated whether C-CPE-PSIF suppresses the spontaneous lung metastasis of 4T1 cells. On day 33, the tumor volume was 1801.2 ± 848.5 mm^3 in the vehicle-treated group and 740.5 ± 94.6 mm^3 in the group treated with 5 μg/kg C-CPE-PSIF (Fig. 3A). The number of lung metastasis colonies was decreased to 2 ± 1 colonies at 5 μg/kg C-CPE-PSIF (Fig. 3B). A dose of 2 μg/kg C-CPE-PSIF did not suppress tumor growth

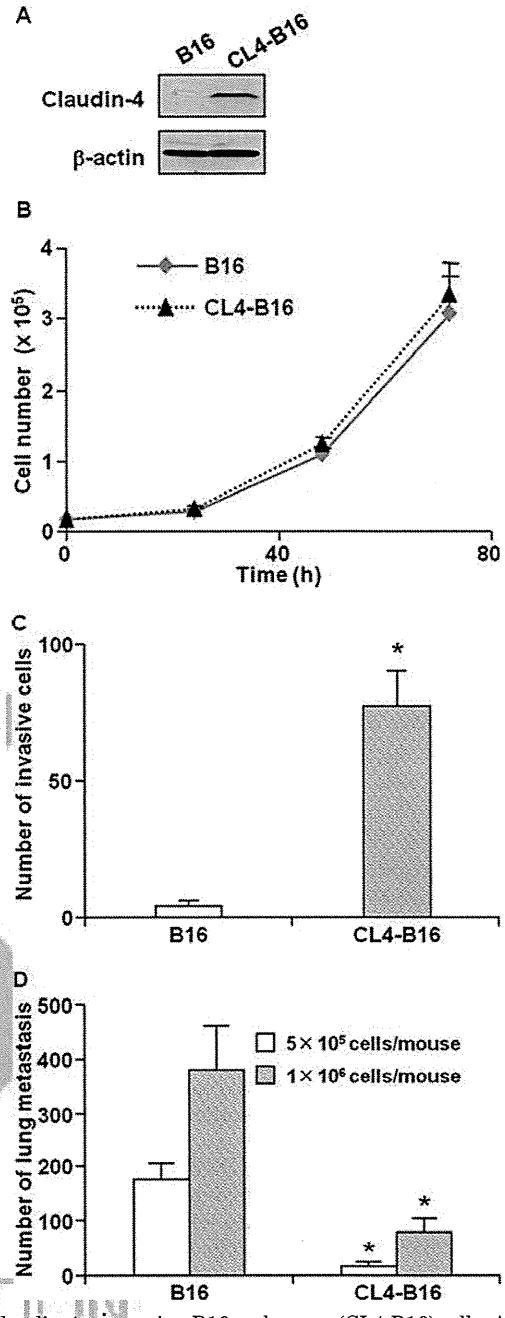

Fig. 1. Claudin-4-expressing B16 melanoma (CL4-B16) cells. A, preparation of CL4-B16 cells. Cell lysates from B16 and CL4-B16 cells were subjected to SDS-polyacrylamide gel electrophoresis, followed by Western blotting with claudin-4 and β-actin. β-Actin is a control for an endogenous protein. B, the effect of claudin-4 on cellular proliferation in B16 cells. B16 or CL4-B16 cells (2×10^4 cells) were seeded onto a 24-well plate. Then, the cell numbers were counted by trypan blue dye exclusion assay at the indicated periods. Data are shown as means ± S.D. ($n = 4$). C, effect of claudin-4 on invasion in B16 cells. B16 or CL4-B16 cells (1×10^5 cells) were seeded into the upper well of the cell culture insert coated with Matrigel. After 24 h, the cells that invaded the bottom membrane of the insert were stained with DiffQuick reagent and counted under a microscope. Data are shown as means ± S.D. ($n = 4$). *, significantly different from B16 cells ($p < 0.01$). D, lung metastasis of CL4-B16 cells. B16 or CL4-B16 cells (5×10^5 or 1×10^6 cells) were injected into the tail veins of mice. After 14 days, the mice were sacrificed, the lungs were fixed, and the colonies on the lung surface were counted. Data are shown as means ± S.D. ($n = 5$). *, significantly different from B16 cells ($p < 0.01$).

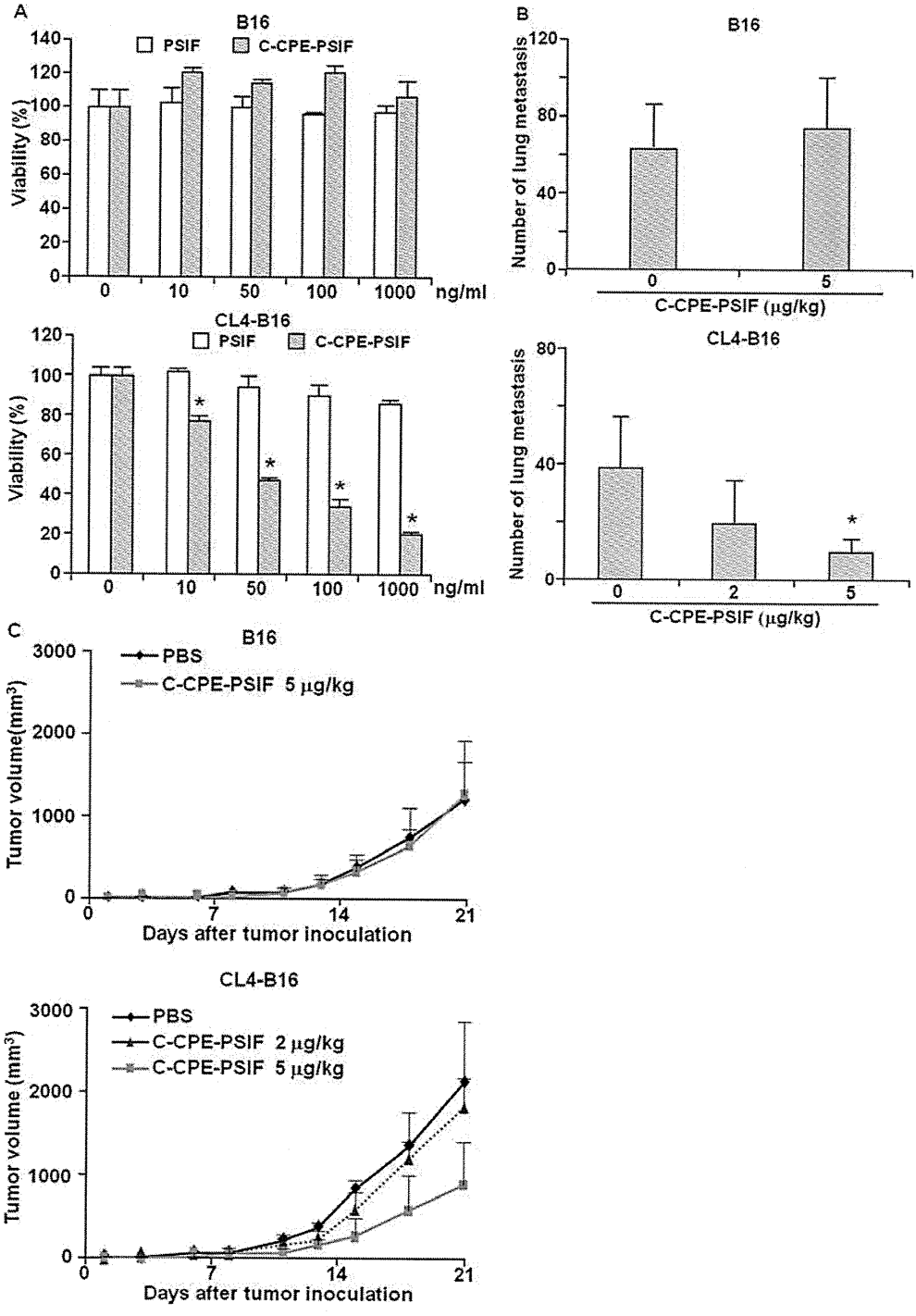

Fig. 2. Antitumor activity of C-CPE-PSIF for CL4-B16 cells. A, cytotoxicity of C-CPE-PSIF in CL4-B16 cells. B16 cells (top) and CL4-B16 cells (bottom) were treated with PSIF or C-CPE-PSIF at the indicated concentrations for 24 h. Cell viability (%) was measured by a WST-8 kit, according to the manufacturer's instructions (Nacalai Tesque). Data represent the mean ± S.D. (n = 3). *, significantly different from the vehicle-treated group ($p < 0.05$). B, antimetastatic activity of C-CPE-PSIF on lung metastasis of B16 (top) or CL4-B16 (bottom) cells. B16 or CL4-B16 cells (1×10^6 cells) were injected into the tail veins of mice on day 0, and vehicle or C-CPE-PSIF (2 or 5 μg/kg) was intravenously injected on days 0, 2, 4, 7, 9, 11, and 13. On day 14, the mice were sacrificed, their lungs were fixed, and the colonies on the lung surface were counted. Data are shown as means ± S.D. (n = 5). *, significantly different from the vehicle-treated group ($p < 0.05$). C, antitumor activity of C-CPE-PSIF on CL4-B16 subcutaneously inoculated allograft. B16 (top) or CL4-B16 (bottom) cells (1×10^5 cells) were intradermally inoculated into the right flank of mice on day 0, and PBS or C-CPE-PSIF (2 or 5 μg/kg) was intravenously injected three times a week. Tumor volume was monitored. Each point is the mean ± S.D. (n = 5). The data are representative of two independent experiments.

but did prevent lung metastasis. The circulating tumor cells might be more sensitive to C-CPE-PSIF than tumor cells in the solid tumor tissue. C-CPE-PSIF treatments did not cause a decrease in body weight (Fig. 3C), and there were no apparent biochemical side effects (Supplemental Fig. 1). ADR, which is frequently used in clinical chemotherapy, suppressed the tumor growth from 970.3 ± 278.4 to 458.6 ± 51.4 mm^3 at 4 mg/kg (Fig. 3D). As shown in Fig. 3E, 4 mg/kg ADR decreased the number of lung metastasis colonies (24 ± 13 colonies in the vehicle-treated group; 6 ± 4 colonies in the ADR-treated group). However, the ADR-treated mice experienced a 26% loss of body weight, which is a sign of side effects (Fig. 3F). Thus, the antitumor activity of C-CPE-PSIF might be more potent than that of ADR. These results indicate that claudin-4-targeting therapy might be a potent strategy for tumor therapy with a low level of side effects and a high level of antitumor activity.

Discussion

Most malignant tumors are derived from the epithelium, and metastasis is the major cause of death from cancers. In the present study, we found that systemic administration of a claudin-targeting molecule suppressed cancer metastasis, indicating that claudin targeting might be an effective therapy against cancer metastasis.

tapraid3/zpt-pt/zpt-pt/zpt00810/zpt9037d10z | xppws | S=1 | 5/15/10 | 1:17 | Art: 168070 | Input-KAF

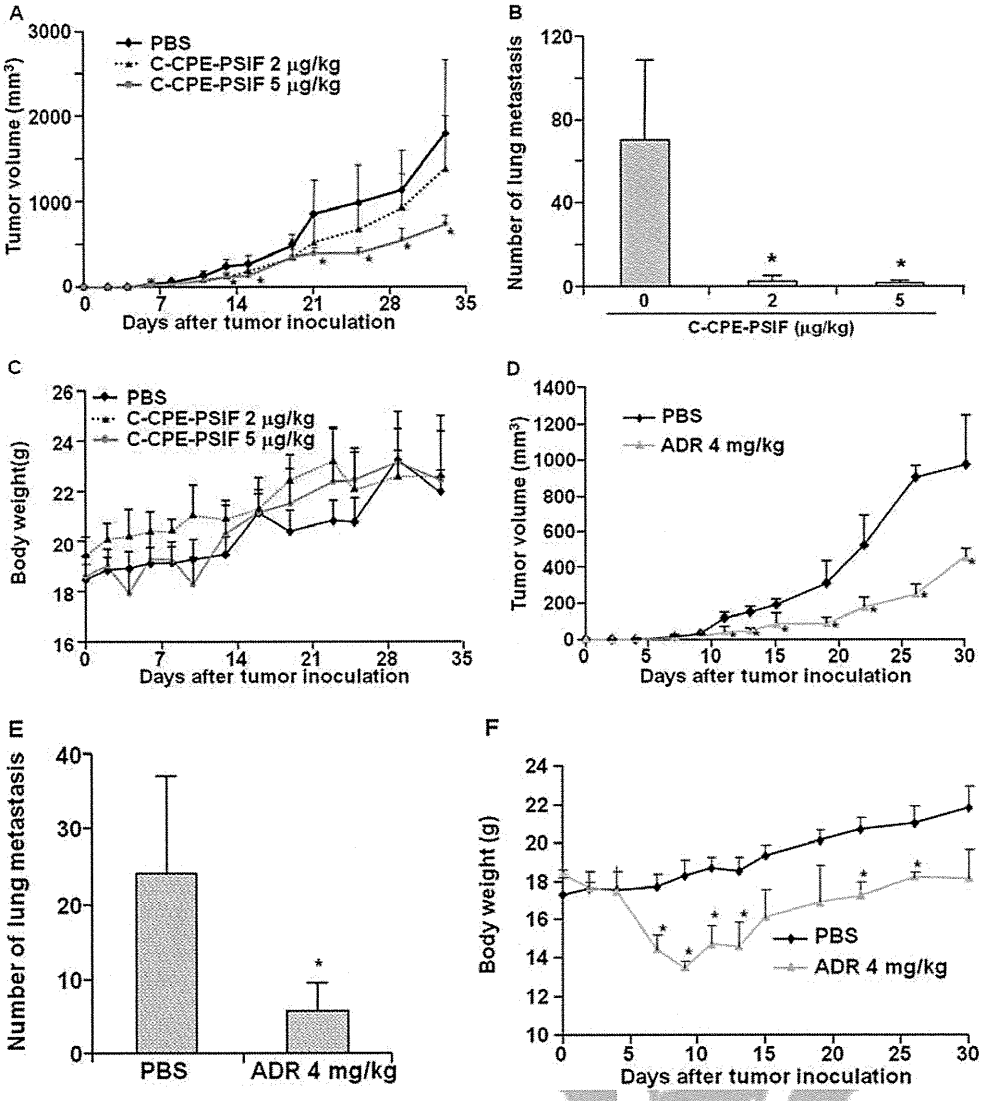

Fig. 3. Antitumor activity of C-CPE-PSIF for murine breast cancer 4T1 cells. 4T1 cells (1×10^5 cells) were intradermally inoculated into the right flanks of mice on day 0, and C-CPE-PSIF (A–C) or ADR (D–F) was intravenously injected three or two times a week at the indicated doses, respectively. Tumor volume (A and D) and body weight (B and E) were monitored. On day 35, the mice were sacrificed, their lungs were stained with India ink, and the number of spontaneous metastases was determined (C and F). Data are shown as means ± S.D. ($n = 5$). *, significantly different from the vehicle-treated group ($p < 0.01$). The data are representative of two independent experiments.

Although the in vitro metastasis activity of CL4-B16 cells was higher than that of parental B16 cells, the in vivo lung metastasis of CL4-B16 cells was lower than that of B16 cells. As shown in Supplemental Fig. 2, claudin-4 increased the invasiveness and migration activity of B16 cells in vitro and decreased lung metastasis in vivo. A possible explanation for this discrepancy might be the experimental model, which evaluates a different stage of metastasis. The migration and invasion activity involved in the early stage of metastasis was investigated in the in vitro analysis, whereas extravasation and colonization to an organ involved in the late stage of metastasis was evaluated by the in vivo experiment. The altered expression of claudin-4 changed the metastasis of 4T1 cells to the heart and liver, suggesting that claudin affects organ-specific metastasis (Erin et al., 2009). Claudin-4 might suppress the lung metastasis of B16 cells.

Claudin is a structural and functional component of TJs (Furuse and Tsukita, 2006). What is the role of claudin in metastasis? Metastasis is composed of three steps: leaving the primary site, entering the blood flow, and invading the distant site. In the first step, the combination of claudin members in the TJ strands may be important. The claudin family contains at least 24 members. Claudin is believed to form homo- and hetero-type claudin strands, and the pattern of the strands differs among tissues and determines the properties of TJ seals (Furuse and Tsukita, 2006). For example, rigid TJ seals were formed when claudin-11 or claudin-15 was exogenously expressed in Madin-Darby canine kidney cells, whereas the expression of claudin-11 or claudin-15 reduced the TJ integrity in LLC-PK1 cells by its dominant negative effects on TJ sealing (Van Itallie et al., 2003). Dominant negative effects of claudin-4 on the TJ barrier might contribute to an acceleration in the detachment of cancer cells from the primary tumor tissue. In the second and third steps of metastasis, cancer cells must move through the extracellular matrix at the primary site and the distant site. Cancer cells must degrade the extracellular matrix by the expression of matrix metalloproteinase and increase their motility. Claudin expression enhanced invasion with increased matrix metalloproteinase activity (Agarwal et al., 2005). There is a relationship between the levels of claudin-1/claudin-4 and the metastasis of human cancers, including hepatic, colonic, ovarian, and gastric cancers (Miwa et al., 2001; Agarwal et al., 2005; Resnick et al., 2005; Halder et al., 2008; Lee et al., 2008). The overexpression of claudin suppressed cancer metastasis in human pancreatic and gastric cancers (Michl et al., 2003; Mima et al., 2005; Ohtani et al., 2009). Claudin-4 suppressed or accelerated in vitro and in

vivo metastasis of human cancer cells (Agarwal et al., 2005; Ohtani et al., 2009). Cell–cell interaction through TJs regulates cell growth signaling (Matter et al., 2005). Taken together, these findings indicate that claudin family members might control several steps of cancer metastasis. The precise molecular mechanism and role of claudin in cancer metastasis remain to be determined.

Whether a claudin-4-targeting method causes severe side effects is critical for its clinical application in cancer therapy. Claudins play pivotal roles in TJ barrier and fence functions by maintaining cellular polarity in normal epithelium (Furuse and Tsukita, 2006). Claudins are believed to be more accessible in tumors than in normal epithelium. Claudins form TJ seals in lateral membranes between adjacent cells in normal epithelium, whereas claudins are exposed on the cell surface during tumorigenesis (Soler et al., 1999; Kominsky, 2006). Indeed, no local or systemic side effects have been observed after the intratumoral administration of CPE (Kominsky et al., 2007; Santin et al., 2007). Here, we also found that the systemic administration of C-CPE-PSIF causes no significant increase in biochemical markers (aspartate aminotransferase, alanine aminotransferase, and blood urea nitrogen) for toxicity at a therapeutic dose of 5 μg/kg (Supplemental Fig. 2). Thus, a claudin-targeting strategy might have weak side effects.

It is difficult to prepare recombinant claudin protein because of its hydrophobic property, and claudin has low antigenicity. Until recently, an antibody against the extracellular loop domain of claudin had never been successfully prepared, and C-CPE was the only known claudin binder. Recently, Romani et al. (2009) prepared a single-chain antibody fragment against claudin-3 by using phage display technology. They found that the antibody fragment binds to ovarian and uterine carcinoma cells in vitro. More importantly, a therapeutic monoclonal antibody against claudin-4 was developed. Suzuki et al. (2009) successfully prepared anticlaudin-4 antibody by immunizing claudin-4-expressing tumor cells into a mouse with autoimmune disease. The antibody mediates antibody-dependent cellular cytotoxicity and both in vitro and in vivo antitumor activity. Although the preparation of anticlaudin antibody may lead to a breakthrough in cancer therapy, the immunogenicity associated with immunotoxin clinical therapies is a future problem (Kreitman and Pastan, 2006). The C-terminal 30 amino acids are the minimum functional domain of C-CPE to bind to claudin-4 (Hanna et al., 1991). The C-terminal 30-amino-acid fragment was used to deliver a cytokine to claudin-4-expressing cells by genetic fusion (Yuan et al., 2009). Humanized antibody and the claudin-4-targeting peptide may be useful for cancer therapy in the near future.

In summary, this is the first report to indicate that systemic injection of a claudin-targeting molecule suppresses tumor growth and metastasis. Hematologic cells do not develop TJs; therefore, a claudin-targeting therapy may have no hematologic toxicity. We anticipate that claudin targeting will be a potent strategy for cancer therapy.

Acknowledgments

We thank members of our laboratory for useful comments and discussion and Drs. Y. Horiguchi (Osaka University, Osaka, Japan), S. Tsunoda (National Institute of Biomedical Innovation, Osaka, Japan), and M. Furuse (Kobe University, Hyogo, Japan) for providing C-CPE cDNA, PSIF cDNA, and claudin cDNA, respectively.

References

Agarwal R, D'Souza T, and Morin PJ (2005) Claudin-3 and claudin-4 expression in ovarian epithelial cells enhances invasion and is associated with increased matrix metalloproteinase-2 activity. *Cancer Res* **65**:7378–7385.

Dhawan P, Singh AB, Deane NG, No Y, Shiou SR, Schmidt C, Neff J, Washington MK, and Beauchamp RD (2005) Claudin-1 regulates cellular transformation and metastatic behavior in colon cancer. *J Clin Invest* **115**:1765–1776.

Erin N, Wang N, Xin P, Bui V, Weisz J, Barkan GA, Zhao W, Shearer D, and Clawson GA (2009) Altered gene expression in breast cancer liver metastases. *Int J Cancer* **124**:1503–1516.

Furuse M and Tsukita S (2006) Claudins in occluding junctions of humans and flies. *Trends Cell Biol* **16**:181–188.

Gupta GP and Massagué J (2006) Cancer metastasis: building a framework. *Cell* **127**:679–695.

Halder SK, Rachakonda G, Deane NG, and Datta PK (2008) Smad7 induces hepatic metastasis in colorectal cancer. *Br J Cancer* **99**:957–965.

Hanna PC, Mietzner TA, Schoolnik GK, and McClane BA (1991) Localization of the receptor-binding region of *Clostridium perfringens* enterotoxin using cloned toxin fragments and synthetic peptides. The 30 C-terminal amino acids define a functional binding region. *J Biol Chem* **266**:11037–11043.

Jemal A, Siegel R, Ward E, Hao Y, Xu J, Murray T, and Thun MJ (2008) Cancer statistics, 2008. *CA Cancer J Clin* **58**:71–96.

Kominsky SL (2006) Claudins: emerging targets for cancer therapy. *Expert Rev Mol Med* **8**:1–11.

Kominsky SL, Tyler B, Sosnowski J, Brady K, Doucet M, Nell D, Smedley JG 3rd, McClane B, Brem H, and Sukumar S (2007) *Clostridium perfringens* enterotoxin as a novel-targeted therapeutic for brain metastasis. *Cancer Res* **67**:7977–7982.

Kominsky SL, Vali M, Korz D, Gabig TG, Weitzman SA, Argani P, and Sukumar S (2004) *Clostridium perfringens* enterotoxin elicits rapid and specific cytolysis of breast carcinoma cells mediated through tight junction proteins claudin 3 and 4. *Am J Pathol* **164**:1627–1633.

Kreitman RJ and Pastan I (2006) Immunotoxins in the treatment of hematologic malignancies. *Curr Drug Targets* **7**:1301–1311.

Lee LY, Wu CM, Wang CC, Yu JS, Liang Y, Huang KH, Lo CH, and Hwang TL (2008) Expression of matrix metalloproteinases MMP-2 and MMP-9 in gastric cancer and their relation to claudin-4 expression. *Histol Histopathol* **23**:515–521.

Martin TA and Jiang WG (2001) Tight junctions and their role in cancer metastasis. *Histol Histopathol* **16**:1183–1195.

Matter K, Aijaz S, Tsapara A, and Balda MS (2005) Mammalian tight junctions in the regulation of epithelial differentiation and proliferation. *Curr Opin Cell Biol* **17**:453–458.

McClane BA and Chakrabarti G (2004) New insights into the cytotoxic mechanisms of *Clostridium perfringens* enterotoxin. *Anaerobe* **10**:107–114.

Michl P, Barth C, Buchholz M, Lerch MM, Rolke M, Holzmann KH, Menke A, Fensterer H, Giehl K, Löhr M, et al. (2003) Claudin-4 expression decreases invasiveness and metastatic potential of pancreatic cancer. *Cancer Res* **63**:6265–6271.

Michl P, Buchholz M, Rolke M, Kunsch S, Löhr M, McClane B, Tsukita S, Leder G, Adler G, and Gress TM (2001) Claudin-4: a new target for pancreatic cancer treatment using *Clostridium perfringens* enterotoxin. *Gastroenterology* **121**:678–684.

Mima S, Tsutsumi S, Ushijima H, Takeda M, Fukuda I, Yokomizo K, Suzuki K, Sano K, Nakanishi T, Tomisato W, et al. (2005) Induction of claudin-4 by nonsteroidal anti-inflammatory drugs and its contribution to their chemopreventive effect. *Cancer Res* **65**:1868–1876.

Mitic LL and Anderson JM (1998) Molecular architecture of tight junctions. *Annu Rev Physiol* **60**:121–142.

Morin PJ (2005) Claudin proteins in human cancer: promising new targets for diagnosis and therapy. *Cancer Res* **65**:9603–9606.

Morita K, Furuse M, Fujimoto K, and Tsukita S (1999) Claudin multigene family encoding four-transmembrane domain protein components of tight junction strands. *Proc Natl Acad Sci USA* **96**:511–516.

Mullin JM (1997) Potential interplay between luminal growth factors and increased tight junction permeability in epithelial carcinogenesis. *J Exp Zool* **279**:484–489.

Ohtani S, Terashima M, Satoh J, Soeta N, Saze Z, Kashimura S, Ohsuka F, Hoshino Y, Kogure M, and Gotoh M (2009) Expression of tight junction-associated proteins in human gastric cancer: down-regulation of claudin-4 correlates with tumor aggressiveness and survival. *Gastric Cancer* **12**:43–51.

Resnick MB, Konkin T, Routhier J, Sabo E, and Pricolo VE (2005) Claudin-1 is a strong prognostic indicator in stage II colonic cancer: a tissue microarray study. *Mod Pathol* **18**:511–518.

Romani C, Comper F, Bandiera E, Ravaggi A, Bignotti E, Tassi RA, Pecorelli S, and Santin AD (2009) Development and characterization of a human single-chain antibody fragment against claudin-3: a novel therapeutic target in ovarian and uterine carcinomas. *Am J Obstet Gynecol* **201**:70,e71–e79.

Saeki R, Kondoh M, Kakutani H, Tsunoda S, Mochizuki Y, Hamakubo T, Tsutsumi Y, Horiguchi Y, and Yagi K (2009) A novel tumor-targeted therapy using a claudin-4-targeting molecule. *Mol Pharmacol* **76**:918–926.

Saiki I (1997) Cell adhesion molecules and cancer metastasis. *Jpn J Pharmacol* **75**:215–242.

Santin AD, Bellone S, Marizzoni M, Palmieri M, Siegel ER, McKenney JK, Hennings L, Comper F, Bandiera E, and Pecorelli S (2007) Overexpression of claudin-3 and claudin-4 receptors in uterine serous papillary carcinoma: novel targets for a type-specific therapy using *Clostridium perfringens* enterotoxin (CPE). *Cancer* **109**:1312–1322.

Santin AD, Cané S, Bellone S, Palmieri M, Siegel ER, Thomas M, Roman JJ, Burnett A, Cannon MJ, and Pecorelli S (2005) Treatment of chemotherapy-resistant human ovarian cancer xenografts in C.B-17/SCID mice by intraperitoneal administration of *Clostridium perfringens* enterotoxin. *Cancer Res* **65**:4334–4342.

Soler AP, Miller RD, Laughlin KV, Carp NZ, Klurfeld DM, and Mullin JM (1999) Increased tight junctional permeability is associated with the development of colon cancer. *Carcinogenesis* **20**:1425–1431.

Sonoda N, Furuse M, Sasaki H, Yonemura S, Katahira J, Horiguchi Y, and Tsukita S (1999) *Clostridium perfringens* enterotoxin fragment removes specific claudins from tight junction strands: Evidence for direct involvement of claudins in tight junction barrier. *J Cell Biol* **147:**195–204.

Staehelin LA (1973) Further observations on the fine structure of freeze-cleaved tight junctions. *J Cell Sci* **13:**763–786.

Steeg PS (2006) Tumor metastasis: mechanistic insights and clinical challenges. *Nat Med* **12:**895–904.

Suzuki M, Kato-Nakano M, Kawamoto S, Furuya A, Abe Y, Misaka H, Kimoto N, Nakamura K, Ohta S, and Ando H (2009) Therapeutic antitumor efficacy of monoclonal antibody against claudin-4 for pancreatic and ovarian cancers. *Cancer Sci* **100:**1623–1630.

Van Itallie CM, Fanning AS, and Anderson JM (2003) Reversal of charge selectivity in cation or anion-selective epithelial lines by expression of different claudins. *Am J Physiol Renal Physiol* **285:**F1078–F1084.

Vermeer PD, Einwalter LA, Moninger TO, Rokhlina T, Kern JA, Zabner J, and Welsh MJ (2003) Segregation of receptor and ligand regulates activation of epithelial growth factor receptor. *Nature* **422:**322–326.

Wodarz A and Näthke I (2007) Cell polarity in development and cancer. *Nat Cell Biol* **9:**1016–1024.

Wong CW, Song C, Grimes MM, Fu W, Dewhirst MW, Muschel RJ, and Al-Mehdi AB (2002) Intravascular location of breast cancer cells after spontaneous metastasis to the lung. *Am J Pathol* **161:**749–753.

Yuan X, Lin X, Manorek G, Kanatani I, Cheung LH, Rosenblum MG, and Howell SB (2009) Recombinant CPE fused to tumor necrosis factor targets human ovarian cancer cells expressing the claudin-3 and claudin-4 receptors. *Mol Cancer Ther* **8:**1906–1915.

Address correspondence to: Dr. Masuo Kondoh, Laboratory of Bio-Functional Molecular Chemistry, Graduate School of Pharmaceutical Sciences, Osaka University, Suita, Osaka 565-0871, Japan. E-mail: masuo@phs.osaka-u.ac.jp

Journal of Controlled Release 149 (2011) 36–41

Contents lists available at ScienceDirect

Journal of Controlled Release

journal homepage: www.elsevier.com/locate/jconrel

Review

Progress in the development of ultrasound-mediated gene delivery systems utilizing nano- and microbubbles

Ryo Suzuki, Yusuke Oda, Naoki Utoguchi, Kazuo Maruyama *

Department of Biopharmaceutics, School of Pharmaceutical Sciences, Teikyo University, 1091-1 Suwarashi, Midori-ku, Sagamihara, Kanagawa 252-5195, Japan

ARTICLE INFO

Article history:
Received 28 December 2009
Accepted 6 May 2010
Available online 12 May 2010

Keywords:
Ultrasound
Microbubbles
Sonoporation
Gene delivery
Cavitation

ABSTRACT

Recently, ultrasound-mediated gene delivery with nano- and microbubbles was developed as a novel non-viral vector system. In this gene delivery system, microstreams and microjets, which are induced by disruption of nano/microbubbles exposed to ultrasound, are used as the driving force to transfer genes into cells by opening transient pores in the cell membrane. This system can directly deliver plasmid DNA and siRNA into cytosol without endocytosis pathway. Therefore, these genes are able to escape from degradation in lysosome and result in enhancing the efficiency of gene expression. In addition, it is expected that ultrasound-mediated gene delivery using nano/microbubbles would be a system to establish non-invasive and tissue specific gene expression because ultrasound can transdermally expose to target tissues and organs. This review focuses on the current ultrasound-mediated gene delivery system using nano/microbubbles. We discuss about the feasibility of this gene delivery system as novel non-viral vector system.

Contents

1. Introduction

Gene therapy has a potential in the treatment of cancer and diseases that are due to genomic causes. Viral vectors are efficient carriers of genes for transduction, but some problems have become evident [1–3]. Delivery vectors that are highly potent in terms of gene transduction efficiency should also be safe and easy to apply. Non-viral vectors have recently received focus as gene carriers, but their transduction efficiency is very low. Efforts have recently been directed towards improving this aspect [4–6]. Towards this end, ultrasound has been investigated for improving the efficiency of transgene delivery, and holds promise as a non-invasive gene delivery system.

Ultrasound shows potential for improving the efficiency of gene delivery into tissues and cells, a technique known as sonophoresis/sonoporation [7]. It is believed that ultrasound perturbs cell membranes and causes transient pores to open in the membrane, thus facilitating gene entry into the cell [8]. In addition, it has been reported that microbubbles utilized as ultrasound contrast agents play an important role in enhancing the efficiency of gene delivery, without causing cell damage [9]. In general, cell damage is dependent on ultrasound intensity, concentration of microbubbles and cell type. Especially, ultrasound intensity and exposure time are key factors. Therefore, it is important to optimize the condition of ultrasound exposure in ultrasound-mediated gene delivery [10–13]. Some researchers studied about the cell damage by the disruption of microbubbles with ultrasound exposure [14–19]. These reports are useful as informative references for ultrasound-mediated gene delivery utilizing microbubbles.

* Corresponding author. Tel.: +81 42 685 3722; fax: +81 42 685 3432.
E-mail address: maruyama@pharm.teikyo-u.ac.jp (K. Maruyama).

0168-3659/$ – see front matter © 2010 Elsevier B.V. All rights reserved.
doi:10.1016/j.jconrel.2010.05.009

Microbubbles which are destroyed by ultrasound exposure generate microstreams or microjets, resulting in shear stress to cells and the generation of transient holes in cell membranes [20]. Since this approach can be used to deliver extracellular molecules such as genes into cells, microbubbles could facilitate ultrasound-mediated gene delivery. In addition, submicron sized bubbles (nanobubbles), which are smaller than conventional microbubbles, were recently reported [21,22], and we have also developed novel liposomal nanobubbles (Bubble liposomes) [11,23–32]. These nanobubbles can also be utilized as enhancing tool of gene delivery efficiency in ultrasound-mediated gene delivery. In this review, we introduced about ultrasound-mediated delivery systems combined with nano/microbubbles and discussed the feasibility as non-viral vector system.

2. Microbubbles as ultrasound contrast agents

Ultrasonography is a widely used diagnostic medical imaging technique that is non-invasive, relatively low-cost, easy to use, provides real-time imaging, and importantly, avoids the use of hazardous ionizing radiation. Ultrasound wave pulses generated by an ultrasound transducer are partially reflected or scattered by the interfaces between different tissues. The transducer detects the ultrasound waves returned by scattering, and these signals are converted to ultrasound images. Since blood scatters ultrasound poorly, ultrasound contrast agents, which increase the scattering and reflection of ultrasound waves, are utilized for blood flow imaging, especially in cardiosonography. Gramiak and Shah in 1968 were the first to use contrast agents in echocardiography [33], and reported that the aortic delineation was improved by intracardiac injection of agitated saline containing air bubbles. However, these air microspheres disappeared within a few seconds following intravenous injection due to the high solubility of air in blood, and the impossibility of larger air bubbles to pass through pulmonary capillaries. For these reasons, it is difficult to use injected conventional air bubbles for opacifying the left cardiac chambers, unless they are injected by the intracoronary or aortic route.

To improve the stability and decrease the size of air bubbles, microbubbles with a thin shell such as albumin (Albunex) or galactose palmitic acid (Levovist) have been developed (Table 1). These bubbles are first-generation microbubbles, and are air-filled microspheres. Their mean diameter ranges from 1 to 8 μm, and they are capable of passing through pulmonary capillaries. However, these air-filled microbubbles disappear from the bloodstream within seconds after administration because of their low resistance to arterial pressure gradients, and the high solubility of air in blood [34]. Approaches for increasing the stability of microbubbles and decreasing the solubility of their gas in blood are clearly required, and lead to the development of microbubbles filled with a high molecular weight hydrophobic gas such as perfluorocarbons or sulfur hexafluoride. These microbubbles represent second-generation contrast agents, in which surfactants, sonicated albumin and phospholipids are used to form the bubble shell in order to improve microbubble stability in the bloodstream. The acoustic backscatter of these microbubbles is higher than that of blood and organs, due to differences in acoustic impedance between gases, and blood or organs. Therefore, microbubbles are useful contrast agents, especially in echocardiography. In addition, Sonazoid which was a phosphatidylserine-stabilized perfluorobutane microbubbles was developed as a useful contrast agent for hepatic tumors [35–37]. This is due to uniqueness of Sonazoid whose microbubbles are likely to be taken up by Kupffer cells (liver macrophages) in the healthy liver and enhances contrast of the liver parenchyma during the delayed phase, which usually occurs within 10 min after the injection. In contrast, tumor that lacks Kupffer cells was not enhanced resulting in clear negative contrast of the tumor [36]. Thus, Sonazoid is a new type of microbubble which is able to target Kupffer cells. However, Sonazoid has been commercially available microbubble for clinical use only in Japan since 2007. In the future, it is expected that tissue specific targeting bubbles such as Sonazoid are developed.

Table 1
Ultrasound contrast agents.

Name	Shell	Entrapping gas	Size (μm)
Albunex	Albumin	Air	4.3
Levovist	Galactose	Air	2–4
Optison	Albumin	Perfluoropropane	3–32
Definity	Lipids	Perfluoropropane	1.1–20
Imagent	Lipids	Perfluoropropane	5
Sonovue	Lipids	Sulphur hexafluoride	2.5
Sonazoid	Lipids	Perfluorobutane	2–3

3. Properties of microbubbles combined with ultrasound

The behavior of microbubbles depends on the amplitude of ultrasound used. At very low acoustic pressure (mechanical index (MI)<0.05–0.1), the microbubbles cause linear oscillation, and the reflected frequency is equal to the transmitted frequency (Fig. 1(a)). An increase in acoustic pressure (0.1<MI<0.3), referred to as low-power imaging, causes non-linear expansion and compression of the microbubbles (Fig. 1(b)). In fact, the bubble becomes somewhat more resistant to compression than to expansion. This phenomenon is known as stable or non-inertial cavitation, and results in the emission of non-linear harmonic signals at multiples of the transmitted frequency [38]. Harmonic imaging with microbubbles enhances the bubbles-to-tissue backscatter signal ratio, due to insignificant harmonic backscatter from tissue in this range of MI. Therefore, this technique can improve the signal-noise ratio and be useful in left ventricular pacification imaging [39]. In addition, stable or non-inertial cavitation can enhance transient cell membrane permeability (Fig. 2(a)) [40]. Machluf et al. reported that ultrasound exposure (0.16 MI, 1 MHz) in the presence of microbubbles deliver plasmid DNA into cells [41,42].

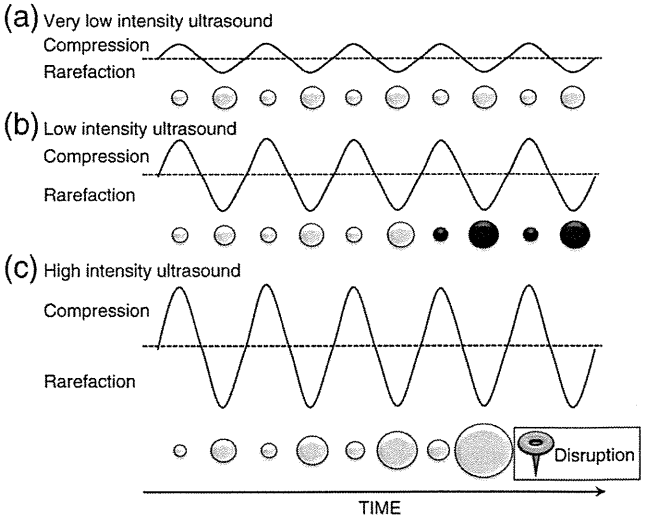

Fig. 1. Scheme showing microbubble behavior in acoustic fields (a) Very low intensity ultrasound induces linear oscillation of the microbubble. (b) Low intensity ultrasound induces oscillation of the microbubble with a gradual increase in microbubble diameter until it reaches a resonant diameter, at which point stable oscillation occurs (filled black circles). (c) High intensity ultrasound causes a rapid increase in the diameter of the microbubble for a few cycles, which induces bubble disruption.

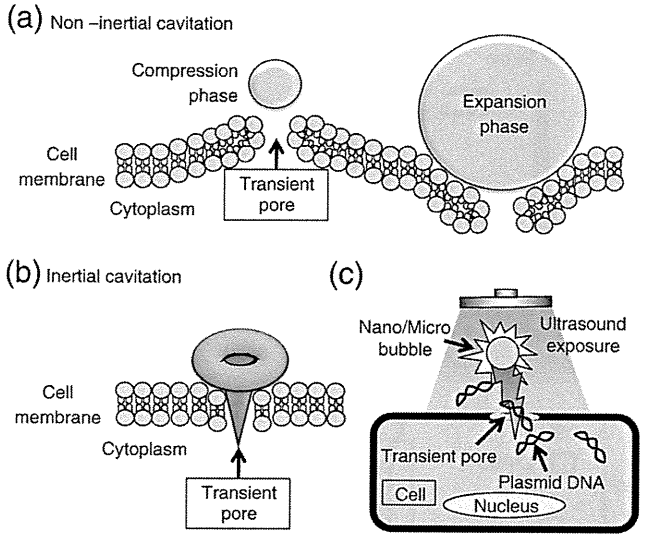

Fig. 2. Scheme showing the pore formation in the cell membrane by oscillating or disrupting microbubble (a) The pushing and pulling behavior (non-inertial cavitation) of the microbubble and (b) the collapse of microbubbles (inertial cavitation) cause rupture of the cell membrane creating pore allowing trans-membrane flux of fluid and macromolecules such as plasmid DNA and oligonucleotides (c).

Higher acoustic pressure (MI>0.3–0.6) causes forced expansion and compression of microbubbles and results in bubble disruption (collapse) (Fig. 1(c)). This inertial cavitation involved in bubble disruption is utilized as flash-replenishment in reperfusion study of diagnosis [43]. This inertial cavitation induces microstreams/microjets around the bubbles. The peak velocity of the microstreams/microjets can reach 700 m/s. These microstreams/microjets can enhance the permeability of cell membranes due to the formation of transient pores (Fig. 2(b)) [20]. In the presence of nano-/microbubbles, the threshold for cavitation decreases, and it results in rendering their destruction feasible at lower energies of ultrasound.

4. Gene delivery using sonoporation as a non-viral vector system

The first studies investigating the utility of ultrasound for gene delivery used frequencies in the range 20–50 kHz [7,44]. However, these frequencies, along with cavitation, are known to cause tissue damage if not properly controlled [45,46]. To overcome this problem, many gene delivery studies have used therapeutic ultrasound, which operates at frequencies of 1–3 MHz, intensities of 0.5–2.5 W/cm^2 or MI 0.3–2, and in pulse-mode [47]. However, as these conditions result in very inefficient gene delivery, therapeutic ultrasound combined with nano/microbubble contrast agents has been investigated for enhancing gene transfection efficiency [9,13,48,49]. This combination method has many of the characteristics required for practical gene therapy including low toxicity, the potential for repeated applications, organ specificity and broad applicability to acoustically accessible organs. Under proper conditions, the combination of ultrasound and nano/microbubbles can create transient non-lethal perforations in cell membranes. Taniyama et al. reported that transient pores formed in cell membranes upon exposure to ultrasound and Optison, and that the pores completely closed [20]. In addition, the behavior of insonated microbubbles was observed with high-speed camera microscopy [50]. Exposure to high intensity ultrasound induced complete disruption of the microbubbles. The above findings suggest that the combination of microbubbles and ultrasound could be useful for gene delivery (Fig. 2(c)).

4.1. Applying to plasmid DNA delivery

Much research has been conducted both *in vitro* and *in vivo* into gene delivery using ultrasound to disrupt microbubbles. In early feasibility studies, reporter genes such as luciferase, β-galactosidase and green fluorescent protein (GFP) were utilized to assess transfection efficiency [13,51–54]. Transfection method in *in vitro* study is very simple. In general, cells suspended with microbubbles and plasmid DNA were exposed with ultrasound for a few second-several tens of seconds due to be completed transfection in a short period of time [27]. Transfection efficiency is affected by ultrasound exposure condition such as intensity, frequency, period, duty cycle, or type and concentration of microbubble [10,11,13,14]. Normally, the efficiency increase according to increasing ultrasound intensity and period [11]. On the other hand, it was reported that the efficiency and cell viability by the transfection with fractionated exposure was higher than that with continuous exposure in the same period of total exposure [19]. In addition, it was reported that there was optimal concentration of microbubbles [55]. Unfortunately, optimal condition is not completely clear in the transfection using this system because of many changeable parameters as mentioned above. Thus, some researchers have studies the properties of this transfection technology to find out optimal condition.

Many of *in vivo* early studies focused on organs and tissues that are readily imaged by diagnostic ultrasonography, including heart [52,56], skeletal muscle [51] and kidney [57]. Bekeredjian et al. reported the use of ultrasound and microbubbles to deliver reporter genes into heart [56]. Subsequently, Korpanty et al. succeeded in delivering the gene for vascular endothelial growth factor (VEGF) into heart using the same gene delivery system, and VEGF-mediated angiogenesis to rat myocardium [58]. This technique has begun to be broadly utilized as a gene delivery system to other organs, tissues and cells such as the vascular system, pancreas, central nerve system, tumors, and hematopoietic cells. For example, Shimamura et al. reported transfection to the central nervous system by sonoporation after injection of a reporter gene and Optison into cistern magna or striatum [59]. In this study, transfection by microbubbles using ultrasound transferred the reporter gene into cells around the neurons, and not into the neuron cells themselves. Takahashi et al. reported gene transfer into the spine using ultrasound and microbubbles [60]. In addition, Aoi et al. developed herpes simplex virus mediated thymidine kinase (HSV-tk)-mediated suicide gene therapy using nanobubbles and ultrasound [61]. In this therapy, HSV-tk corded plasmid DNA and nanobubbles were injected into tumor tissue of mice, and ultrasound was transdermally exposed toward the tissue. The reduction of tumor size was observed by administration of ganciclovir in the mice transfected HSV-tk corded plasmid DNA with nanobubbles and ultrasound. Previously, we developed novel liposomal nanobubble (Bubble liposome) entrapping perfluoropropane gas (Fig. 3(a–c)) [11,27]. The size of Bubble liposomes was about 500 nm and they were much smaller than Sonazoid (Fig. 3(b)). Bubble liposome could also utilize as an effective plasmid DNA delivery tool *in vitro* (Fig. 3(d)) and *in vivo* by the combination with ultrasound. We reported the utility of Bubble liposome in cancer gene therapy using interleukin-12 (IL-12) corded plasmid DNA [24]. The combination of Bubble liposomes and ultrasound dramatically suppressed tumor growth (Fig. 4). As mentioned above, sonoporation combined with nano/microbubbles could be a good system for plasmid DNA delivery.

4.2. Applying to oligonucleotide delivery

Oligonucleotides such as antisense, decoy and small interfering RNA (siRNA) are important molecules that can stop the expression of specific genes [62,63]. In particular, RNA interference (RNAi) using siRNA has potential in the development of new treatments for disease,

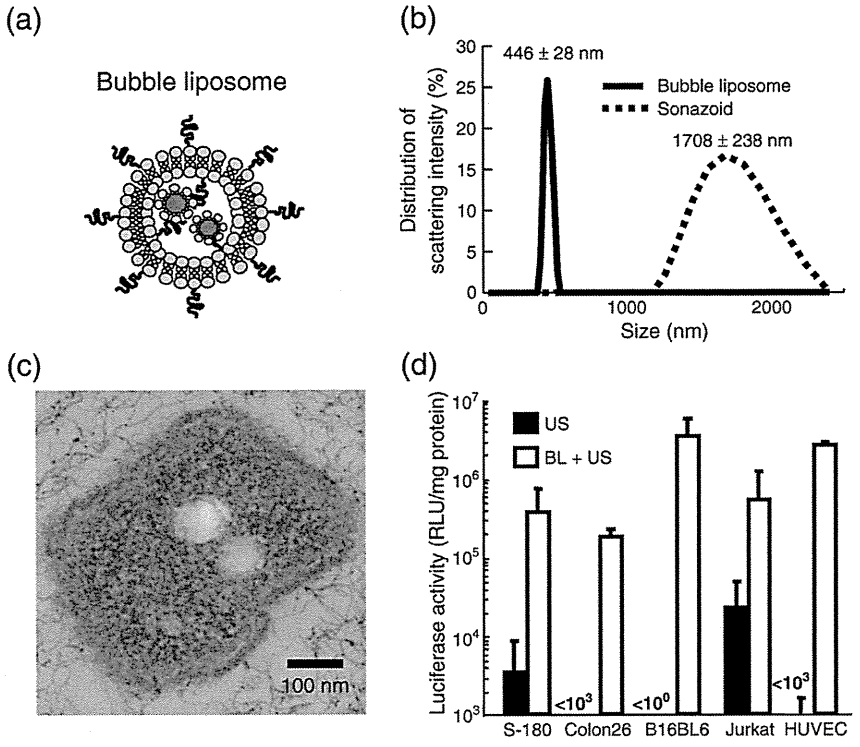

Fig. 3. Comparison of microbubbles and Bubble liposomes (a) Schematic of Bubble liposome. (b) Size distribution of Sonazoid and Bubble liposomes as measured by dynamic light scattering. (c) Transmission electron microscopy (50,000×) of Bubble liposome. (d) Luciferase expression in various types of cells transfected using Bubble liposomes and ultrasound. Cells (1×10^5 cells/500 μL) mixed with pCMV-Luc (5 μg) and Bubble liposomes (60 μg) were exposed or not to ultrasound (frequency, 2 MHz; duty, 50%; burst rate, 2 Hz; intensity, 2.5 W/cm^2; time 10 s). The cells were washed and cultured for 2 days. Thereafter, luciferase activity was determined with luminometer. Data are shown as means ± S.D. ($n=3$). BL, Bubble liposome, pCMV-Luc: luciferase corded plasmid DNA, HUVEC: human umbilical vascular endothelial cell.

including malignant, infectious and autoimmune diseases. In order to achieve efficient gene silencing, it is important that the siRNA is introduced into the cytoplasm of the target cell [64]. Diverse approaches have been attempted to develop efficient oligonucleotide delivery methods [62]. However, technologies that enable the tissue-targeted delivery of siRNA using non-viral vectors need improvement.

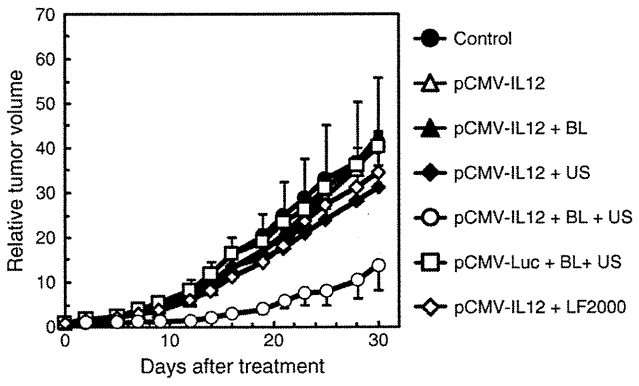

Fig. 4. Cancer gene therapy by IL-12 gene delivery with Bubble liposomes and ultrasound B6C3F1 mice were intradermally inoculated with 1×10^6 OV-HM cells into the flank. On day 7 after tumor inoculation, the tumors were injected with pCMV-IL12 (10 μg) using Bubble liposomes (2.5 μg) and/or ultrasound (1 MHz, 0.7 W/cm^2, 1 min), or Lipofectamine 2000 as a conventional lipofection method. (b) Therapeutic effect was assessed by measuring tumor growth. The volume of the growing tumors was calculated by: (tumor volume; mm^3) = (major axis; mm) × (minor axis; mm)^2 × 0.5). The data are represented as tumor volume relative to the tumor volume on day 7 after tumor inoculation. Each point represents the mean ± SD ($n=5$). BL: Bubble liposomes, US: Ultrasound, LF2000: Lipofectamine 2000, pCMV-IL-12: IL-12 corded plasmid DNA, pCMV-Luc: Luciferase corded plasmid DNA.

As mentioned above, the combination of ultrasound and nano/microbubbles can directly deliver extracellular molecules into the cytosol [25], where antisense, decoy and siRNA function, so this delivery system might better exhibit the functions of these oligonucleotides. Azuma et al. reported that NF-κB decoy delivery into transplanted kidney by the combination of microbubbles and ultrasound could significantly decrease IL-1β and TNF-α (inflammatory cytokines) and prolonged the survival rate of kidney-transplanted mice [57]. Negishi et al. reported that siRNA was directly introduced into the cytoplasm by nanobubbles and ultrasound [30]. In addition, transfection of siRNA into tibialis muscles with nanobubble and ultrasound resulted in gene-silencing, which was sustained for more than 3 weeks. It therefore appears that the combination of nano/microbubbles and ultrasound could be a useful siRNA delivery system. In addition, siRNA transfection with ultrasound and microbubbles was utilized to apply to mesenchymal stem cells, indicating that this technique could be applicable to genetically modified stem cell therapy. Vandenbroucke et al. also developed an interesting siRNA delivery system using sonoporation [65]. They coupled (PEG-siPlex) of PEGylated cationic liposomes and siRNA, and introduced the complex into gas-filled lipid microbubbles. Both the microbubbles and PEG-siPlex, which were modified with biotin, were attached via avidin. Although PEG-siPlex can protect siRNA from digestion by nucleases *in vivo*, PEGylation makes it difficult for the siRNA to be recognized and taken up by the target cells. The microbubble/sonication system should be able to overcome the negative effects of PEGylating siRNA-cationic liposomes (siPlex) and enhance the efficiency of ultrasound-assisted siRNA delivery. Although siRNA delivery mediated by ultrasound and nano/microbubbles must be optimized, this system may open up new perspectives for ultrasound-controlled *in vivo* siRNA delivery.

5. Efforts to tissue- or organ-selective gene delivery

To establish ideal gene therapy, it is important to deliver therapeutic gene into target tissue or organ. In the early study, gene and nano/microbubbles were directly injected into target tissue and organ [53,66]. However, in this method, there are some limitations such as injection volume and injection technique. To improve these problems, some researchers recently developed ultrasound-mediated gene delivery by the supplying gene and nano/microbubbles via blood flow [11,67]. In this delivery, gene expression was limited in the area exposed ultrasound. Ultrasound can be easily focused to a target tissue or organ. Therefore, it might be possible to develop an optimal tissue- or organ-specific gene delivery system by combining nano/microbubble targeting and focused ultrasound. Shen et al. succeeded to developed ultrasound-mediated gene expression in liver via intraportal injection of plasmid DNA and microbubbles [68]. Grayburn et al. reported insulin expression following insulin gene delivery to pancreatic islets in rat by a combination of microbubbles and ultrasound exposure and succeeded to decrease blood glucose level in diabetes rat [67,69]. We also developed the gene delivery into tumor tissue by the combination of injection from tumor dominant artery and ultrasound exposure toward tumor tissue [11]. In addition, transdermal ultrasound exposure toward liver could induce liver selective gene expression after systemic injection of plasmid DNA and Bubble liposomes. In this case, luciferase expression was dominantly observed in the parenchymal cells of liver. These results suggested that Bubble liposomes could quickly transduce plasmid DNA into each tissue by cavitation even under the existence of blood stream. Moreover, we developed the combination method using mannosylated lipoplexes and Bubble liposomes with ultrasound to enhance gene transfection in mannose receptor-expressing cells in liver [29]. In this study, after systemic injection of mannosylated lipoplex, Bubble liposomes were systemically injected and ultrasound was transdermally exposed toward liver. Gene expression was observed mannose receptor-expressing cells such as macrophage and dendritic cells which were known as antigen presenting cells. It is expected that ultrasound-mediated gene delivery with nano/microbubbles might be useful to develop target tissue or organ-selective gene delivery in vivo.

Previously, several groups have reported active targetable nano/microbubbles to endothelium [70], rejected tissues [71], neovasculature endothelium [72], lymph node-related vasculature [73] and activated platelets[74] by targeting ICAM-1 [75], VCAM-1 [76] or integrins [77]. We also developed blood clot targetable Bubble liposomes modified with arginine-glycine-aspartic acid (RGD) peptides to develop effective ultrasound contrast agents for blood clots imaging [78]. Although these nano/microbubbles were developed as ultrasound imaging agents, it might be possible to develop an optimal tissue- or organ-selective gene delivery system by combining targetable nano/microbubble associated with gene and ultrasound.

6. Conclusion

Ultrasound has long been utilized as a useful diagnostic tool. Therapeutic ultrasound was recently developed and is being utilized in clinical settings. The combination of therapeutic ultrasound and nano/microbubbles is an interesting and important system for establishing a novel and non-invasive gene delivery system. Gene expression efficiency with this system can effectively deliver gene compared with conventional non-viral vector system such as lipofection method due to deliver gene into cytosol without endocytosis pathway. Many *in vivo* studies has been reported about ultrasound-mediated gene delivery with nano/microbubbles. Especially, there are some reports about feasibility studies of gene therapy for various diseases [24,29,61,67] In addition, this system has a potency of site specific gene delivery by the control of ultrasound exposure site. Therefore, it is expected that this technology would be utilized as a novel gene delivery system in clinical field.

References

[1] E. Check, Safety panel backs principle of gene-therapy trials, Nature 420 (2002) 595.
[2] E. Check, Second cancer case halts gene-therapy trials, Nature 421 (2003) 305.
[3] E. Marshall, Gene therapy death prompts review of adenovirus vector Science 286 (1999) 2244–2245.
[4] K. Kogure, H. Akita, Y. Yamada, H. Harashima, Multifunctional envelope-type nano device (MEND) as a non-viral gene delivery system, Adv. Drug Deliv. Rev. 60 (2008) 559–571.
[5] F. Liu, C.C. Conwell, X. Yuan, L.M. Shollenberger, L. Huang, Novel nonviral vectors target cellular signaling pathways: regulated gene expression and reduced toxicity, J. Pharmacol. Exp. Ther. 321 (2007) 777–783.
[6] K. Itaka, S. Ohba, K. Miyata, H. Kawaguchi, K. Nakamura, T. Takato, U.I. Chung, K. Kataoka, Bone regeneration by regulated in vivo gene transfer using biocompatible polyplex nanomicelles, Mol. Ther. 15 (2007) 1655–1662.
[7] M. Fechheimer, J.F. Boylan, S. Parker, J.E. Sisken, G.L. Patel, S.G. Zimmer, Transfection of mammalian cells with plasmid DNA by scrape loading and sonication loading, Proc. Natl. Acad. Sci. U. S. A. 84 (1987) 8463–8467.
[8] M.W. Miller, D.L. Miller, A.A. Brayman, A review of in vitro bioeffects of inertial ultrasonic cavitation from a mechanistic perspective, Ultrasound Med. Biol. 22 (1996) 1131–1154.
[9] W.J. Greenleaf, M.E. Bolander, G. Sarkar, M.B. Goldring, J.F. Greenleaf, Artificial cavitation nuclei significantly enhance acoustically induced cell transfection, Ultrasound Med. Biol. 24 (1998) 587–595.
[10] L.B. Feril Jr., R. Ogawa, K. Tachibana, T. Kondo, Optimized ultrasound-mediated gene transfection in cancer cells, Cancer Sci. 97 (2006) 1111–1114.
[11] R. Suzuki, T. Takizawa, Y. Negishi, N. Utoguchi, K. Sawamura, K. Tanaka, E. Namai, Y. Oda, Y. Matsumura, K. Maruyama, Tumor specific ultrasound enhanced gene transfer in vivo with novel liposomal bubbles, J. Control. Release 125 (2008) 137–144.
[12] S.V. Pislaru, C. Pislaru, R.R. Kinnick, R. Singh, R. Gulati, J.F. Greenleaf, R.D. Simari, Optimization of ultrasound-mediated gene transfer: comparison of contrast agents and ultrasound modalities, Eur. Heart J. 24 (2003) 1690–1698.
[13] T. Li, K. Tachibana, M. Kuroki, M. Kuroki, Gene transfer with echo-enhanced contrast agents: comparison between Albunex, Optison, and Levovist in mice–initial results, Radiology 229 (2003) 423–428.
[14] M.A. Hassan, M.A. Buldakov, R. Ogawa, Q.L. Zhao, Y. Furusawa, N. Kudo, T. Kondo, P. Riesz, Modulation control over ultrasound-mediated gene delivery: evaluating the importance of standing waves, J. Control. Release 141 (2010) 70–76.
[15] D.J. Wells, Electroporation and ultrasound enhanced non-viral gene delivery in vitro and in vivo, Cell Biol. Toxicol. 26 (2010) 21–28.
[16] M.A. Hassan, L.B. Feril Jr., K. Suzuki, N. Kudo, K. Tachibana, T. Kondo, Evaluation and comparison of three novel microbubbles: enhancement of ultrasound-induced cell death and free radicals production, Ultrason. Sonochem. 16 (2009) 372–378.
[17] L.B. Feril Jr., T. Kondo, Q.L. Zhao, R. Ogawa, K. Tachibana, N. Kudo, S. Fujimoto, S. Nakamura, Enhancement of ultrasound-induced apoptosis and cell lysis by echo-contrast agents, Ultrasound Med. Biol. 29 (2003) 331–337.
[18] N. Kudo, K. Okada, K. Yamamoto, Sonoporation by single-shot pulsed ultrasound with microbubbles adjacent to cells, Biophys. J. 96 (2009) 4866–4876.
[19] D.P. Guo, X.Y. Li, P. Sun, Y.B. Tang, X.Y. Chen, Q. Chen, L.M. Fan, B. Zang, L.Z. Shao, X.R. Li, Ultrasound-targeted microbubble destruction improves the low density lipoprotein receptor gene expression in HepG2 cells, Biochem. Biophys. Res. Commun. 343 (2006) 470–474.
[20] Y. Taniyama, K. Tachibana, K. Hiraoka, T. Namba, K. Yamasaki, N. Hashiya, M. Aoki, T. Ogihara, K. Yasufumi, R. Morishita, Local delivery of plasmid DNA into rat carotid artery using ultrasound, Circulation 105 (2002) 1233–1239.
[21] Z. Gao, A.M. Kennedy, D.A. Christensen, N.Y. Rapoport, Drug-loaded nano/microbubbles for combining ultrasonography and targeted chemotherapy, Ultrasonics 48 (2008) 260–270.
[22] Y. Wang, X. Li, Y. Zhou, P. Huang, Y. Xu, Preparation of nanobubbles for ultrasound imaging and intracelluar drug delivery, Int. J. Pharm. 384 (2010) 148–153.
[23] R. Suzuki, K. Maruyama, Effective in vitro and in vivo gene delivery by the combination of liposomal bubbles (bubble liposomes) and ultrasound exposure, Methods Mol. Biol. 605 (2009) 473–486.
[24] R. Suzuki, E. Namai, Y. Oda, N. Nishiie, S. Otake, R. Koshima, K. Hirata, Y. Taira, N. Utoguchi, Y. Negishi, S. Nakagawa, K. Maruyama, Cancer gene therapy by IL-12 gene delivery using liposomal bubbles and tumoral ultrasound exposure, J. Control. Release 142 (2010) 245–250.
[25] R. Suzuki, Y. Oda, N. Utoguchi, E. Namai, Y. Taira, N. Okada, N. Kadowaki, T. Kodama, K. Tachibana, K. Maruyama, A novel strategy utilizing ultrasound for antigen delivery in dendritic cell-based cancer immunotherapy, J. Control. Release 133 (2009) 198–205.
[26] R. Suzuki, T. Takizawa, Y. Kuwata, M. Mutoh, N. Ishiguro, N. Utoguchi, A. Shinohara, M. Eriguchi, H. Yanagie, K. Maruyama, Effective anti-tumor activity of oxaliplatin encapsulated in transferrin-PEG-liposome, Int. J. Pharm. 346 (2008) 143–150.
[27] R. Suzuki, T. Takizawa, Y. Negishi, K. Hagisawa, K. Tanaka, K. Sawamura, N. Utoguchi, T. Nishioka, K. Maruyama, Gene delivery by combination of novel liposomal bubbles with perfluoropropane and ultrasound, J. Control. Release 117 (2007) 130–136.
[28] R. Suzuki, T. Takizawa, Y. Negishi, N. Utoguchi, K. Maruyama, Effective gene delivery with liposomal bubbles and ultrasound as novel non-viral system, J. Drug Target. 15 (2007) 531–537.

[29] K. Un, S. Kawakami, R. Suzuki, K. Maruyama, F. Yamashita, M. Hashida, Enhanced transfection efficiency into macrophages and dendritic cells by a combination method using mannosylated lipoplexes and bubble liposomes with ultrasound exposure, Hum. Gene Ther. 21 (2010) 65–74.

[30] Y. Negishi, Y. Endo, T. Fukuyama, R. Suzuki, T. Takizawa, D. Omata, K. Maruyama, Y. Aramaki, Delivery of siRNA into the cytoplasm by liposomal bubbles and ultrasound, J. Control. Release 132 (2008) 124–130.

[31] Y. Negishi, D. Omata, H. Iijima, Y. Takabayashi, K. Suzuki, Y. Endo, R. Suzuki, K. Maruyama, M. Nomizu, Y. Aramaki, Enhanced laminin-derived peptide AG73-mediated liposomal gene transfer by bubble liposomes and ultrasound, Mol. Pharm. 7 (2010) 217–226.

[32] T. Yamashita, S. Sonoda, R. Suzuki, N. Arimura, K. Tachibana, K. Maruyama, T. Sakamoto, A novel bubble liposome and ultrasound-mediated gene transfer to ocular surface: RC-1 cells in vitro and conjunctiva in vivo, Exp. Eye Res. 85 (2007) 741–748.

[33] P.M. Shah, R. Gramiak, D.H. Kramer, P.N. Yu, Determinants of atrial (S4) and ventricular (S3) gallop sounds in primary myocardial disease, N Engl J. Med. 278 (1968) 753–758.

[34] A. Kabalnov, D. Klein, T. Pelura, E. Schutt, J. Weers, Dissolution of multicomponent microbubbles in the bloodstream: 1, Theory Ultrasound Med Biol 24 (1998) 739–749.

[35] K. Yanagisawa, F. Moriyasu, T. Miyahara, M. Yuki, H. Iijima, Phagocytosis of ultrasound contrast agent microbubbles by Kupffer cells, Ultrasound Med. Biol. 33 (2007) 318–325.

[36] R. Watanabe, M. Matsumura, T. Munemasa, M. Fujimaki, M. Suematsu, Mechanism of hepatic parenchyma-specific contrast of microbubble-based contrast agent for ultrasonography: microscopic studies in rat liver, Invest. Radiol. 42 (2007) 643–651.

[37] K. Korenaga, M. Korenaga, M. Furukawa, T. Yamasaki, I. Sakaida, Usefulness of Sonazoid contrast-enhanced ultrasonography for hepatocellular carcinoma: comparison with pathological diagnosis and superparamagnetic iron oxide magnetic resonance images, J. Gastroenterol. 44 (2009) 733–741.

[38] E.C. Unger, E. Hersh, M. Vannan, T.O. Matsunaga, T. McCreery, Local drug and gene delivery through microbubbles, Prog. Cardiovasc. Dis. 44 (2001) 45–54.

[39] S.L. Mulvagh, A.N. DeMaria, S.B. Feinstein, P.N. Burns, S. Kaul, J.G. Miller, M. Monaghan, T.R. Porter, L.J. Shaw, F.S. Villanueva, Contrast echocardiography: current and future applications, J. Am. Soc. Echocardiogr. 13 (2000) 331–342.

[40] A. van Wamel, K. Kooiman, M. Harteveld, M. Emmer, F.J. ten Cate, M. Versluis, N. de Jong, Vibrating microbubbles poking individual cells: drug transfer into cells via sonoporation, J. Control. Release 112 (2006) 149–155.

[41] M. Duvshani-Eshet, L. Baruch, E. Kesselman, E. Shimoni, M. Machluf, Therapeutic ultrasound-mediated DNA to cell and nucleus: bioeffects revealed by confocal and atomic force microscopy, Gene Ther. 13 (2006) 163–172.

[42] M. Duvshani-Eshet, D. Adam, M. Machluf, The effects of albumin-coated microbubbles in DNA delivery mediated by therapeutic ultrasound, J. Control. Release 112 (2006) 156–166.

[43] K. Kalantarinia, J.T. Belcik, J.T. Patrie, K. Wei, Real-time measurement of renal blood flow in healthy subjects using contrast-enhanced ultrasound, Am. J. Physiol. Ren. Physiol 297 (2009) F1129–F1134.

[44] M. Joersbo, J. Brunstedt, Protein synthesis stimulated in sonicated sugar beet cells and protoplasts, Ultrasound Med. Biol. 16 (1990) 719–724.

[45] H.R. Guzman, A.J. McNamara, D.X. Nguyen, M.R. Prausnitz, Bioeffects caused by changes in acoustic cavitation bubble density and cell concentration: a unified explanation based on cell-to-bubble ratio and blast radius, Ultrasound Med. Biol. 29 (2003) 1211–1222.

[46] W. Wei, B. Zheng-zhong, W. Yong-jie, Z. Qing-wu, M. Ya-lin, Bioeffects of low-frequency ultrasonic gene delivery and safety on cell membrane permeability control, J. Ultrasound Med. 23 (2004) 1569–1582.

[47] H.J. Kim, J.F. Greenleaf, R.R. Kinnick, J.T. Bronk, M.E. Bolander, Ultrasound-mediated transfection of mammalian cells, Hum. Gene Ther. 7 (1996) 1339–1346.

[48] D.M. Hallow, A.D. Mahajan, T.E. McCutchen, M.R. Prausnitz, Measurement and correlation of acoustic cavitation with cellular bioeffects, Ultrasound Med. Biol. 32 (2006) 1111–1122.

[49] R.V. Shohet, S. Chen, Y.T. Zhou, Z. Wang, R.S. Meidell, R.H. Unger, P.A. Grayburn, Echocardiographic destruction of albumin microbubbles directs gene delivery to the myocardium, Circulation 101 (2000) 2554–2556.

[50] A. van Wamel, A. Bouakaz, M. Versluis, N. de Jong, Micromanipulation of endothelial cells: ultrasound-microbubble-cell interaction, Ultrasound Med. Biol. 30 (2004) 1255–1258.

[51] J.P. Christiansen, B.A. French, A.L. Klibanov, S. Kaul, J.R. Lindner, Targeted tissue transfection with ultrasound destruction of plasmid-bearing cationic microbubbles, Ultrasound Med. Biol. 29 (2003) 1759–1767.

[52] S. Chen, R.V. Shohet, R. Bekeredjian, P. Frenkel, P.A. Grayburn, Optimization of ultrasound parameters for cardiac gene delivery of adenoviral or plasmid deoxyribonucleic acid by ultrasound-targeted microbubble destruction, J. Am. Coll. Cardiol. 42 (2003) 301–308.

[53] Q.L. Lu, H.D. Liang, T. Partridge, M.J. Blomley, Microbubble ultrasound improves the efficiency of gene transduction in skeletal muscle in vivo with reduced tissue damage, Gene Ther. 10 (2003) 396–405.

[54] S. Tsunoda, O. Mazda, Y. Oda, Y. Iida, S. Akabame, T. Kishida, M. Shin-Ya, H. Asada, S. Gojo, J. Imanishi, H. Matsubara, T. Yoshikawa, Sonoporation using microbubble BR14 promotes pDNA/siRNA transduction to murine heart, Biochem. Biophys. Res. Commun. 336 (2005) 118–127.

[55] Y. Taniyama, K. Tachibana, K. Hiraoka, M. Aoki, S. Yamamoto, K. Matsumoto, T. Nakamura, T. Ogihara, Y. Kaneda, R. Morishita, Development of safe and efficient novel nonviral gene transfer using ultrasound: enhancement of transfection efficiency of naked plasmid DNA in skeletal muscle, Gene Ther. 9 (2002) 372–380.

[56] R. Bekeredjian, S. Chen, P.A. Frenkel, P.A. Grayburn, R.V. Shohet, Ultrasound-targeted microbubble destruction can repeatedly direct highly specific plasmid expression to the heart, Circulation 108 (2003) 1022–1026.

[57] H. Azuma, N. Tomita, Y. Kaneda, H. Koike, T. Ogihara, Y. Katsuoka, R. Morishita, Transfection of NFkappaB-decoy oligodeoxynucleotides using efficient ultrasound-mediated gene transfer into donor kidneys prolonged survival of rat renal allografts, Gene Ther. 10 (2003) 415–425.

[58] G. Korpanty, S. Chen, R.V. Shohet, J. Ding, B. Yang, P.A. Frenkel, P.A. Grayburn, Targeting of VEGF-mediated angiogenesis to rat myocardium using ultrasonic destruction of microbubbles, Gene Ther. 12 (2005) 1305–1312.

[59] M. Shimamura, N. Sato, Y. Taniyama, S. Yamamoto, M. Endoh, H. Kurinami, M. Aoki, T. Ogihara, Y. Kaneda, R. Morishita, Development of efficient plasmid DNA transfer into adult rat central nervous system using microbubble-enhanced ultrasound, Gene Ther. 11 (2004) 1532–1539.

[60] M. Takahashi, K. Kido, A. Aoi, H. Furukawa, M. Ono, T. Kodama, Spinal gene transfer using ultrasound and microbubbles, J. Control. Release 117 (2007) 267–272.

[61] A. Aoi, Y. Watanabe, S. Mori, M. Takahashi, G. Vassaux, T. Kodama, Herpes simplex virus thymidine kinase-mediated suicide gene therapy using nano/microbubbles and ultrasound, Ultrasound Med. Biol. 34 (2008) 425–434.

[62] E. Fattal, G. Barratt, Nanotechnologies and controlled release systems for the delivery of antisense oligonucleotides and small interfering RNA, Br. J. Pharmacol. 157 (2009) 179–194.

[63] S. Kimura, K. Egashira, L. Chen, K. Nakano, E. Iwata, M. Miyagawa, H. Tsujimoto, K. Hara, R. Morishita, K. Sueishi, R. Tominaga, K. Sunagawa, Nanoparticle-mediated delivery of nuclear factor kappaB decoy into lungs ameliorates monocrotaline-induced pulmonary arterial hypertension, Hypertension 53 (2009) 877–883.

[64] K. Tiemann, J.J. Rossi, RNAi-based therapeutics-current status, challenges and prospects EMBO, Mol. Med. 1 (2009) 142–151.

[65] R.E. Vandenbroucke, I. Lentacker, J. Demeester, S.C. De Smedt, N.N. Sanders, Ultrasound assisted siRNA delivery using PEG-siPlex loaded microbubbles, J. Control. Release 126 (2008) 265–273.

[66] C.H. Miao, A.A. Brayman, K.R. Loeb, P. Ye, L. Zhou, P. Mourad, L.A. Crum, Ultrasound enhances gene delivery of human factor IX plasmid, Hum. Gene Ther. 16 (2005) 893–905.

[67] S. Chen, J.H. Ding, R. Bekeredjian, B.Z. Yang, R.V. Shohet, S.A. Johnston, H.E. Hohmeier, C.B. Newgard, P.A. Grayburn, Efficient gene delivery to pancreatic islets with ultrasonic microbubble destruction technology, Proc. Natl. Acad. Sci. U. S. A. 103 (2006) 8469–8474.

[68] Z.P. Shen, A.A. Brayman, L. Chen, C.H. Miao, Ultrasound with microbubbles enhances gene expression of plasmid DNA in the liver via intraportal delivery, Gene Ther. 15 (2008) 1147–1155.

[69] R. Chai, S. Chen, J. Ding, P.A. Grayburn, Efficient, glucose responsive and islet-specific transgene expression by a modified rat insulin promoter, Gene Ther. 16 (2009) 1202–1209.

[70] F.S. Villanueva, R.J. Jankowski, S. Klibanov, M.L. Pina, S.M. Alber, S.C. Watkins, G.H. Brandenburger, W.R. Wagner, Microbubbles targeted to intercellular adhesion molecule-1 bind to activated coronary artery endothelial cells, Circulation 98 (1998) 1–5.

[71] G.E. Weller, E. Lu, M.M. Csikari, A.L. Klibanov, D. Fischer, W.R. Wagner, F.S. Villanueva, Ultrasound imaging of acute cardiac transplant rejection with microbubbles targeted to intercellular adhesion molecule-1, Circulation 108 (2003) 218–224.

[72] D.B. Ellegala, H. Leong-Poi, J.E. Carpenter, A.L. Klibanov, S. Kaul, M.E. Shaffrey, J. Sklenar, J.R. Lindner, Imaging tumor angiogenesis with contrast ultrasound and microbubbles targeted to alpha(v)beta3, Circulation 108 (2003) 336–341.

[73] P. Hauff, M. Reinhardt, A. Briel, N. Debus, M. Schirner, Molecular targeting of lymph nodes with L-selectin ligand-specific US contrast agent: a feasibility study in mice and dogs, Radiology 231 (2004) 667–673.

[74] P.A. Schumann, J.P. Christiansen, R.M. Quigley, T.P. McCreery, R.H. Sweitzer, E.C. Unger, J.R. Lindner, T.O. Matsunaga, Targeted-microbubble binding selectively to GPIIb IIIa receptors of platelet thrombi, Invest. Radiol. 37 (2002) 587–593.

[75] G.E. Weller, F.S. Villanueva, E.M. Tom, W.R. Wagner, Targeted ultrasound contrast agents: in vitro assessment of endothelial dysfunction and multi-targeting to ICAM-1 and sialyl Lewisx, Biotechnol. Bioeng. 92 (2005) 780–788.

[76] C.Z. Behm, B.A. Kaufmann, C. Carr, M. Lankford, J.M. Sanders, C.E. Rose, S. Kaul, J.R. Lindner, Molecular imaging of endothelial vascular cell adhesion molecule-1 expression and inflammatory cell recruitment during vasculogenesis and ischemia-mediated arteriogenesis, Circulation 117 (2008) 2902–2911.

[77] J.R. Lindner, Detection of inflamed plaques with contrast ultrasound, Am. J. Cardiol. 90 (2002) 32L–35L.

[78] K. Hagisawa, N.T., K. Iida, H. Luo, R.J. Siegel, Thrombolysis using low frequency ultrasound with activated platelet targeting bubble liposome in a rabbit iliac artery, Circulation 112 (Sup.II) (2005) 503.

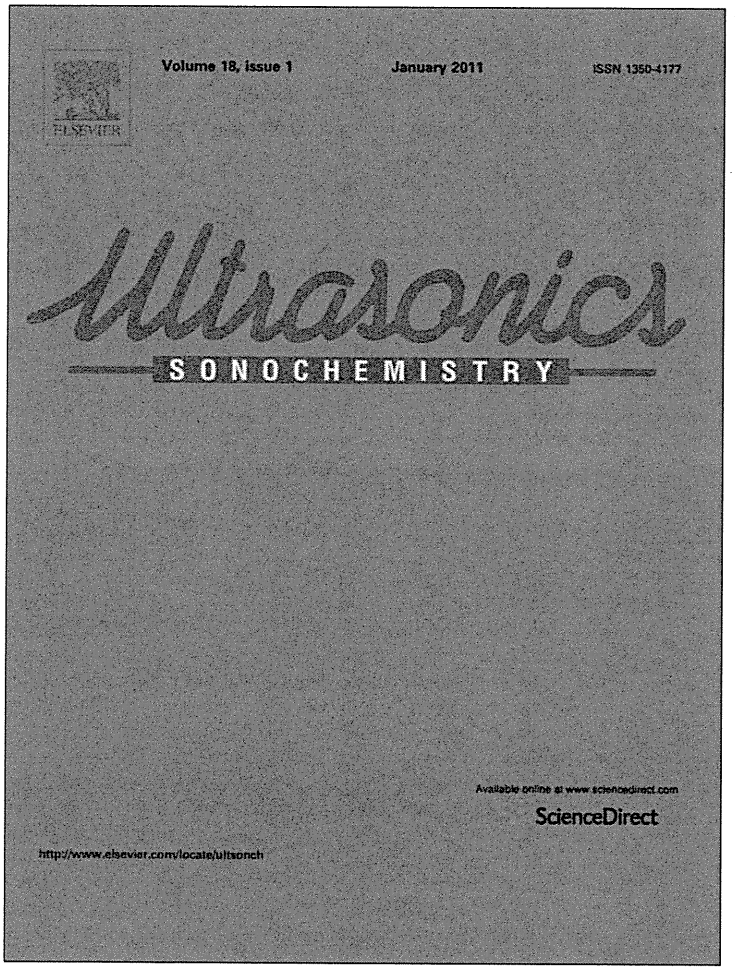

Ultrasonics Sonochemistry 18 (2011) 425–430

Contents lists available at ScienceDirect

Ultrasonics Sonochemistry

journal homepage: www.elsevier.com/locate/ultsonch

Synergistic effect of ultrasound and antibiotics against *Chlamydia trachomatis*-infected human epithelial cells in vitro

Yurika Ikeda-Dantsuji [a], Loreto B. Feril Jr. [a,*], Katsuro Tachibana [a], Koichi Ogawa [a], Hitomi Endo [a], Yoshimi Harada [a], Ryo Suzuki [b], Kazuo Maruyama [b]

[a] Department of Anatomy, Fukuoka University School of Medicine, Fukuoka, Japan
[b] Department of Biopharmaceutics, School of Pharmaceutical Sciences, Teikyo University, Kanagawa, Japan

ARTICLE INFO

Article history:
Received 12 April 2010
Received in revised form 12 July 2010
Accepted 21 July 2010
Available online 27 July 2010

Keywords:
Ultrasound
Nanobubbles
Antibiotic
Intracellular bacteria

ABSTRACT

To investigate whether or not the combined ultrasound and antibiotic treatment is effective against chlamydial infection, a new ultrasound exposure system was designed to treat chlamydia-infected cells. First, the minimum inhibitory concentrations of antibiotics against *Chlamydia trachomatis* were determined. Infected cultures were treated with antibiotics then sonicated at intensity of 0.15 or 0.44 W/cm^2 with or without Bubble liposomes. After 48 or 72 h after infection, chlamydial inclusions were stained and examined by fluorescence microscopy. The internalization of dextran–fluorescein conjugates by ultrasound irradiation with Bubble liposomes was observed by fluorescence microscopy. The results showed that application of nanobubble-enhanced ultrasound caused no significant effect on cell viability and chlamydial infectivity. However, Doxycycline (1/2 MIC) or CZX (1.0 μg/ml) in combination with nanobubble-enhanced ultrasound dramatically reduced the number of inclusions compared with that administered with antibiotics only. Bubble dose-dependent synergy was also observed. After ultrasound irradiation at intensity of 0.44 W/cm^2 on the presence of Bubble liposomes, 10% of HeLa cells were observed to have internalized the dextran molecules. This study suggests the possibility of using nanobubble-enhanced ultrasound to deliver antibiotic molecules into cells to eradiate intracellular bacteria, such as chlamydiae, without causing much damage to the cells itself.

1. Introduction

An obligate intracellular pathogen, *Chlamydia trachomatis*, is the most prevalent sexually transmitted bacterium worldwide [1]. *C. trachomatis* is a Gram-negative bacterium which has a unique biphasic developmental cycle characterized by an infectious but metabolically inactive extracellular form, called the 'elementary body', which initiates infection through the uptake by the host cell. Thereafter, elementary bodies differentiate into noninfectious but metabolically active forms, called the 'reticulate body', which proliferate within the inclusion. Reticulate bodies also differentiate back to elementary bodies before release at the end of the developmental cycle. At its sites of primary infection, *C. trachomatis* infects the urethral or cervical epithelium, causing acute urethritis or cervicitis [2]. These frequently progress into chronic inflammatory disease, the most significant of which, is chronic salpingitis, an inflammatory disease of fallopian tubes that can result in pelvic inflammatory disease, ectopic pregnancy, and tubal infertility [3].

The recommended antibiotic treatments for urogenital infections are a single dose of azithromycin or a 7-day course of doxycycline for management of active infections [4]. These regimens have been shown to result in satisfactory cure rates of acute infections [5,6]; however, chronic diseases (designated "persistent infection") have been suggested to be less responsive to antibiotic therapy [7].

Previous work has shown that some antibiotics treatment of *Pseudomonas aeruginosa* or *Escherichia coli* coupled with ultrasound irradiation enhances the bactericidal activity [8]. The more recent research has revealed that similar synergistic effects of combined ultrasound and antibiotic treatment are seen in both Gram-positive and Gram-negative bacteria with some antibiotics, especially the aminoglycosides [9]. It is not clear whether the combined ultrasound and antibiotic treatment are effective on intracellular pathogen, e.g. chlamydial infection. If an intracellular bacterial infection could be efficiently eradicated from an infected person, one could avoid chronic antibiotic treatments. In addition, this strategy of treatment could be beneficial in the management of chlamydial persistent diseases.

Here, we are studying the synergistic use of ultrasound and antibiotics to kill the *chlamydia*. This report presents results of

* Corresponding author. Address: 7-45-1 Nanakuma, Jonan-ku, Fukuoka 814-0180 Japan. Tel.: +81 92 801 1011x3206; fax: +81 92 865 6032.
E-mail addresses: ferilism@yahoo.com, feril@fukuoka-u.ac.jp (L.B. Feril).

1350-4177/$ - see front matter © 2010 Elsevier B.V. All rights reserved.
doi:10.1016/j.ultsonch.2010.07.015

the first step in that research, which is investigation of the in vitro response of *C. trachomatis*-infected human epithelial cells to combination of ultrasound and two types of antibiotics.

2. Materials and methods

2.1. Chlamydial strain and cell lines

C. trachomatis serovar E/UW-5/Cx was prepared in McCoy cells and propagated according to a previously reported method [10]. The mouse fibroblast cell line McCoy cell (CRL 1696) and human epithelial cell line HeLa 229 cell (CLL 2.1) were maintained in Dulbecco's modified Eagle medium (DMEM, Invitrogen, Grand Island, NY, USA) supplemented with 10% heat-inactivated fetal calf serum (FCS, Invitrogen) and 100 μg/ml streptomycin.

2.2. Infection of HeLa cells

The HeLa cells were seeded into a 24-well plate with lumox™ fluorocarbon film base (optically clear, 50 μm-thin, gas permeable film, Greiner bio-one, Gottingen, Germany). Stocks of chlamydial strain were diluted with sucrose–phosphate–glutamate (SPG) medium [10]. Chlamydial suspensions of 0.5×10^4 inclusion-forming units (IFUs) in 0.25 ml SPG medium were inoculated onto the monolayer cultures of HeLa cells (1×10^4 cells/well). This is equivalent to a multiplicity of infection of 0.5. After incubation at 37 °C for 90 min, the inoculum was decanted, and the cells were washed in medium to remove the nonadsorbed chlamydiae and were then further incubated in 1 ml DMEM containing 1 μg/ml cycloheximide (Sigma Chemicals, St. Louis, MO, USA) and 2% FCS (maintenance medium).

2.3. Preparation of bubble liposome

Bubble liposomes were prepared according to a method previously described [11]. Liposomes composed of 1,2-distearoyl-sn-glycero-phosphatidylcholine (DSPC) (NOF Corp., Tokyo, Japan) and 1,2-distearoyl-snglycero-3-phosphatidyl-ethanolamine-methoxypolyethyleneglycol(DSPE-PEG(2k)-OMe, (PEG Mw = ca. 2000), NOF) (94: 6 (m/m)) were prepared by reverse phase evaporation. Briefly, all reagents (totallipid: 100 μmol) were dissolved in 8 ml of 1:1 (v/v) chloroform/diisopropyl ether, then 4 ml of phosphate buffered saline (PBS) were added. The mixture was sonicated and evaporated at 65 °C. The solvent was completely removed, and the size of the liposomes was adjusted to less than 200 nm using an extruding apparatus (Northern Lipids Inc., Vancouver, BC, Canada) and sizing filters (pore sizes: 100 and 200 nm; Nuclepore Track-Etch Membrane, Whatman plc, UK). After sizing, the liposomes were sterilized by passing them through a 0.45 μm pore size filter (MILLEX HV filter unit, Durapore PVDF membrane, Millipore Corp., MA, USA). The size of the liposomes was measured by dynamic light scattering (ELS-800, Otsuka Electronics Co., Ltd., Osaka, Japan). The average diameter of these liposomes was between 150 and 200 nm. Lipid concentration was measured using the Phospholipid C test (Wako Pure Chemical Industries). BLs were prepared from the liposomes and perfluoropropane gas (Takachiho Chemical Industrial Co., Ltd., Tokyo, Japan). Briefly, 5 ml sterilized vials containing 2 ml of the liposome suspension (lipid concentration: 2 mg/ml) were filled with perfluoropropane, capped, and then supercharged with 7.5 ml of perfluoropropane. The vial was placed in a bath-type sonicator (42 kHz, 100 W; BRANSONIC 2510J-DTH, Branson Ultrasonics Co., Danbury, CT, USA) for 5 min to form the BLs. In this method, the liposomes were reconstituted by sonication under the condition of supercharge with perfluoropropane in the 5 ml vial container. At the same time, perfluoropropane would be entrapped within lipids like micelles, which were made by DSPC and DSPE-PEG(2k)-OMe from liposome composition, to form nanobubbles. The lipid nanobubbles were encapsulated within the reconstituted liposomes, which sizes were changed into around 1 μm from 150 to 200 nm of original.

2.4. Immunofluorescence staining and fluorescence microscopy

At 48 or 72 h after infection, the infected monolayers were washed with PBS, and the cells were fixed with −20 °C chilled methanol. After the specimens had been dried, the inclusion bodies were stained with fluorescein isothiocyanate (FITC)-labeled monoclonal antibody against *C. trachomatis* lipopolysaccharides (Progen Biotechnik, Heidelberg, Germany) for 30 min at room temperature. The cells were rinsed with saline, and the films were cut off from the plate, and mounted in a 1:1 solution of PBS–glycerol. The antibody staining resulted in yellow–green chlamydial proteins, and Evans blue counterstaining yielded red eukaryotic cells. The formation of inclusions was assessed using a Zeiss Axiophot fluorescence microscope. The cells positive for inclusions are considered infected cells and infectivity was presented as the number of inclusion-forming units (IFUs).

2.5. Antibiotics and measurements of MICs

Doxycycline (DOX, Sigma Chemicals) and ceftizoxime (CZX, Fujisawa Yakuhin Kogyou, Tokyo, Japan) were obtained in powder form. Both antibiotics were diluted with saline, and were dissolved in maintenance medium at a concentration of 100 μg/ml and frozen at −80 °C until used. The minimum inhibitory concentrations (MICs) were determined using a method previously described [12]. Briefly, confluent monolayer cultures of cells in a 24-well flat-bottomed plate with 13-mm coverslips were inoculated by centrifugation and incubated in 1 ml of maintenance medium containing a serial dilution of antibiotics for 72 h. To determine the MICs, the cover slips were stained and observed as described in Immunofluorescence staining and fluorescence microscopy. The lowest concentration of the antimicrobial agent that completely inhibited the formation of visible chlamydial inclusions was determined as the MIC.

2.6. Ultrasound exposure

An acoustically transparent gel (Pharmaceutical Innovations Inc., Newark, NJ) was applied on the ultrasound probe before positioning the plate containing the sample on top of it (Fig. 1). Thera-

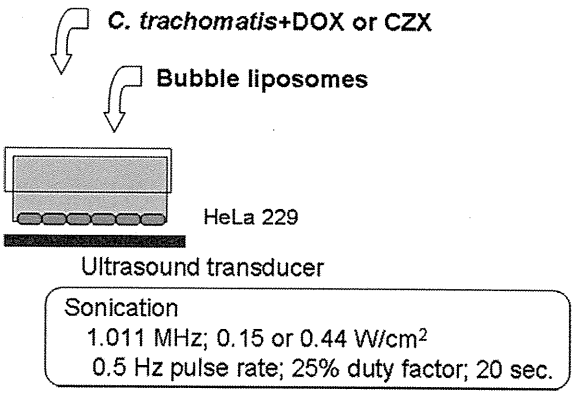

Fig. 1. Experimental design. Schematic drawing of the ultrasound setting. *C. trachomatis*-infected HeLa cells were exposed to ultrasound after addition of antibiotic and Bubble liposomes.

peutic ultrasound (1.011 MHz) was irradiated from a device (Sono-Pore KTAC-4000, NepaGene, Chiba, Japan) at intensity of 0.15 or 0.44 W/cm^2 (duty cycle of 25%) for 20 s immediately after addition of Bubble liposomes into the sample.

2.7. Measurement of cell viability

The Trypan blue dye exclusion test was carried out by mixing 200 μl of the suspension of HeLa cells with an equal amount of 0.3% Trypan blue solution (Sigma Chemicals) in PBS. After 5 min incubation at room temperature, the number of cells excluding Trypan blue was counted using a C-Chip disposable hemocytometer (Digital Bio Technology Co., Gyeonggi, Korea) to estimate the number of viable cells immediately after sonication.

2.8. Measurement of infectivity of chlamydiae

The 1.0 ml of chlamydial suspensions in SPG treated with ultrasound and/or nanobubbles was inoculated into triplicate cultures of McCoy cells in order to estimate the infectivity immediately after sonication. Chlamydial suspensions, 0.25 ml each, were added onto the monolayer culture of McCoy cells. After centrifugation at 1000*g* for 60 min, the inoculum was decanted, and the cells were washed with medium to remove the nonadsorbed chlamydiae, and were then further incubated in 1.0 ml of maintenance medium.

2.9. Internalization of dextran–fluorescein conjugates

Dextran–fluorescein conjugates (3000 MW, anionic: Molecular Probes, Inc., OR, USA) were soluble in 0.02 M Tris–HCl buffer (pH 8.0) at 10 μg/ml, and performed by filtration using 0.2 μm pore-diameter sterile filters. Aqueous solutions of dextran were diluted to 10 μg/ml with maintenance medium. The 50 μl of solution of dextran conjugates instead of antibiotics were added into the monolayer cultures of HeLa cells in a 24-well plate with lumox™ fluorocarbon film bottom. Ultrasound was irradiated for 20 s with or without Bubble liposomes at 50 μg/ml. Cultures were rinsed in PBS(−) solution and examined immediately after rinsing by fluorescent microscopy (Leica Microsystems CTR4000, Wetzlar, Germany).

2.10. Statistical analysis

Data from these study were analyzed using unpaired *t*-test including Welch's correction. Results were considered to be significant when the corrected *p*-value is less than 0.05, indicated as $p < 0.05$ in the manuscript and figure legends. Error bars shown in the figures are standard deviations of duplicate samples in experiments repeated at least three times.

3. Results

3.1. Cell viability of HeLa cells and infectivity of chlamydiae by nanobubble-enhanced ultrasound

We first investigated whether nanobubble-enhanced ultrasound decreased the cell viability of HeLa cells and the infectivity of *chlamydia*. As shown in Table 1, ultrasound at intensity of 0.44 W/cm^2 caused no significant effect, but ultrasound at intensity of 0.15 W/cm^2 decreased slightly on cell viability. On the other hand, the application of ultrasound also caused no significant effect on chlamydial infectivity at both intensities of 0.15 and 0.44 W/cm^2 (Fig. 2).

Table 1
Viable cell counts following exposure of HeLa cell to ultrasound.

Application of ultrasound	Cytotoxicity: No. of viable cells/well (% of control)
Control	
(−) Sonication	7475 ± 1950
(−) Bubble liposomes	(100)
Bubble	
(−) Sonication	8940 ± 950
(+) Bubble liposomes	(120)
Ultrasound (0.15 W/cm^2)	6290 ± 950
(+) Bubble liposomes	(84)
Ultrasound (0.44 W/cm^2)	7865 ± 950
(+) Bubble liposomes	(105)

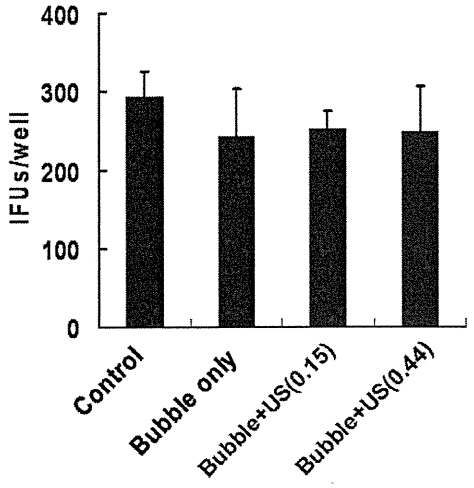

Fig. 2. Infectivity of chlamydiae by nanobubble-enhanced ultrasound. No significant change in infectivity when cells were treated with bubble liposomes (Bubble only) or ultrasound at intensities 0.15 W/cm^2 (Bubble + US(0.15)) and 0.44 W/cm^2 (Bubble + US(0.44)) in the presence of bubble liposomes.

3.2. Ultrasonic enhancement of antibiotic action on C. trachomatis-infected HeLa cells

The MIC of DOX for *C. trachomatis*-infected HeLa cells was determined to be 0.03 μg/ml. Infected cultures were treated with DOX at 1/2 MIC (0.015 μg/ml) then sonicated with or without the addition of Bubble liposomes (50 μg/ml). The results showed that ultrasound alone or Bubble liposomes alone did not decrease the formation of inclusions in infected cells administered with DOX (Fig. 3). However, DOX at 1/2 MIC in combination with nanobubble-enhanced ultrasound significantly reduced the number of IFUs to 66 ± 39% and 15 ± 12%, respectively, at intensities of 0.15 and 0.44 W/cm^2, compared with that administered with DOX at 1/2 MIC only (Control in Fig. 3).

The MIC of CZX for *C. trachomatis*-infected HeLa cells could not be determined because intracellular pathogens are known to be resistant to CZX, therefore, we tried to use considerably high concentrations of 0.125, 0.25, 0.5 and 1.0 μg/ml. Any of the concentrations used did not show any effect against chlamydia when applied alone but in combination with bubble-enhanced ultrasound, significant IFU reduction was observed and most with 1.0 μg/ml CZX (data not shown). Similar to the observed effect with DOX, 1.0 μg/ml CZX in combination with nanobubble-enhanced ultrasound also reduced the number of IFUs to 53 ± 32% and 50 ± 48%, respectively, at intensities of 0.15 and 0.44 W/cm^2, compared with that administered 1.0 μg/ml CZX only (Fig. 4).

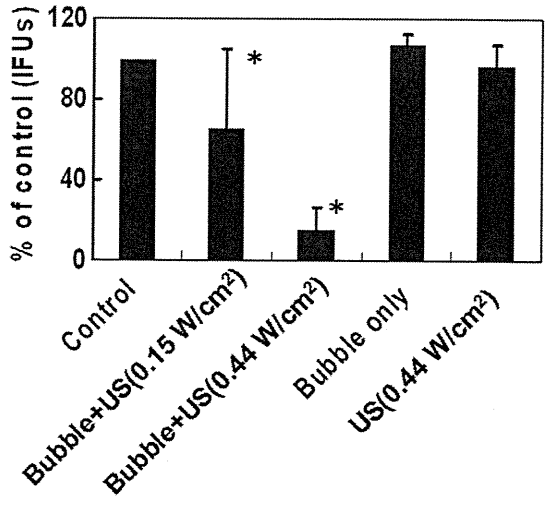

Fig. 3. Ultrasonic enhancement of bactericidal activity of doxycycline (DOX) at 1/2 MIC on *C. trachomatis*-infected HeLa cells. Data represents % of control that is the number of chlamydial inclusions treated with DOX at 1/2 MIC only (*$p < 0.05$).

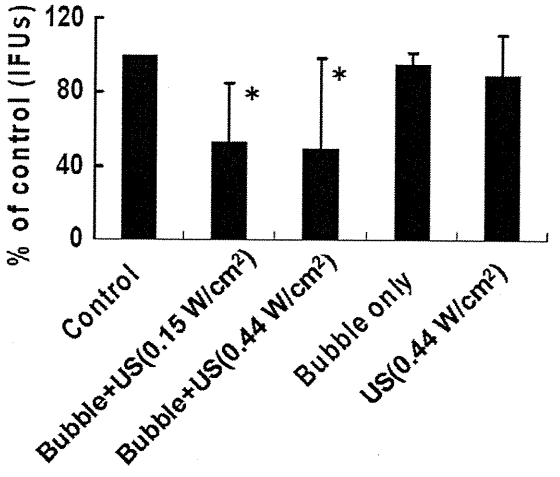

Fig. 4. Ultrasonic enhancement of bactericidal activity of ceftizoxime (CZX) at 1.0 μg/ml on *C. trachomatis*-infected HeLa cells. Data represents % of control that is the number of chlamydial inclusions treated with CZX at 1.0 μg/ml only (*$p < 0.05$).

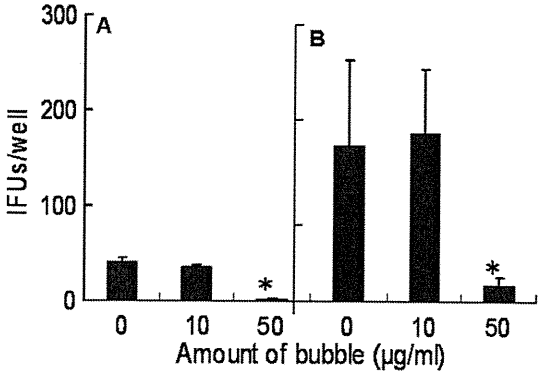

Fig. 5. Effect of concentration of Bubble liposomes in addition with ultrasound irradiation and antibiotics on *C. trachomatis*-infected HeLa cells. (A) Before ultrasound irradiation, the infected culture was treated with DOX at 1/2 MIC. (B) Before ultrasound irradiation, the infected culture was treated with CZX at 1.0 μg/ml (*$p < 0.05$).

Next, we examined the effect of the amount of Bubble liposomes on nanobubble-enhanced ultrasound reduction of IFU. With increased amount of Bubble liposomes, the synergistic effect of ultrasound and DOX was significantly increased (Fig. 5A). Bubble dose-dependent synergy was also observed with CZX and ultrasound (Fig. 5B).

3.3. Internalization of dextran–fluorescein conjugates by ultrasound

Finally, to examine whether ultrasound can facilitate intracellular uptake of large molecules, we sonicated HeLa cells in the presence of fluorescein-labeled dextran and afterwards examined the cells by fluorescence microscopy. Approximately 10% of viable cells were observed to have internalized the dextran molecules after ultrasound irradiation at intensity of 0.44 W/cm^2 in the presence of Bubble liposomes (Fig. 6). This observation showed that ultrasound can facilitate cellular uptake of large molecules.

4. Discussion

Previous reports have shown a synergistic effect between ultrasound and antibiotics in killing *E. coli* and *P. aeruginosa* [8]. The purpose of this present study was to determine if the same synergistic effect could be observed with *C. trachomatis* even if this is an intracellular organism. The results of the MIC experiments and the measurements of bactericidal activity against *C. trachomatis* show that addition of nanobubble-enhanced ultrasound to DOX treatment enhanced the effectiveness of DOX in eradicating *C. trachomatis* (Fig. 3). Dramatic reduction of IFUs to 15 ± 12% was observed at higher ultrasound intensity of 0.44 W/cm^2 (Fig. 3). These findings could have important clinical applications because the tissue concentration of antibiotics often became below the MICs in actual clinical settings.

In a previous study, the duration of the illness in patients with *C. trachomatis*-triggered reactive arthritis (ReA) was shorter in patients treated with lymecycline for 3 months than in a placebo-treated group [13]. Other studies on the long-term treatment of acute ReA with ciprofloxacin showed no advantage over placebo treatment in the outcome of ReA [14]. So far, the optimal treatment of ReA with antimicrobial drugs remains controversial. In addition, it was recently reported that persistent chlamydial infection induced ReA [15–17]. Most recent finding by Reveneau et al. have shown that persistent chlamydial forms are more resistant to DOX than acute forms because of the decreased antibiotic uptake by host cells [18]. Therefore, a more effective treatment of persistent chlamydial infections requires a method to increase antibiotics uptake by the infected cells. On the other hand, advances in ultrasound and nanobubble-enhanced ultrasound technologies have raised the possibility of using ultrasound not only for diagnostic but also for therapeutic purposes. The combination of an agent as nanobubbles and ultrasound exposure makes sonoporation possible. Sonoporation is characterized by a transient change in cellular membrane permeability mediated by ultrasound [19–24]; the cavitation energy created by the bubble collapse is thought to be the key mechanism [19]. Thereby, we confirmed that the intracellular delivery of macromolecules such as dextran was observed under the condition used in our experiments (Fig. 6). In addition, ultrasound did not damage HeLa cells or chlamydial organisms in the presence of Bubble liposomes (Fig. 2 and Table 1). This may be due to the size of the bubbles such that cavitations created are enough to deliver the drug to the cells but not "large" enough to create fatal damage to the cell itself. However, to understand the dynamic of the interactions between nanobubble, cell membrane and ultrasound [25], further study is needed. Collectively, our data suggest the possibility of using nanobubble-en-

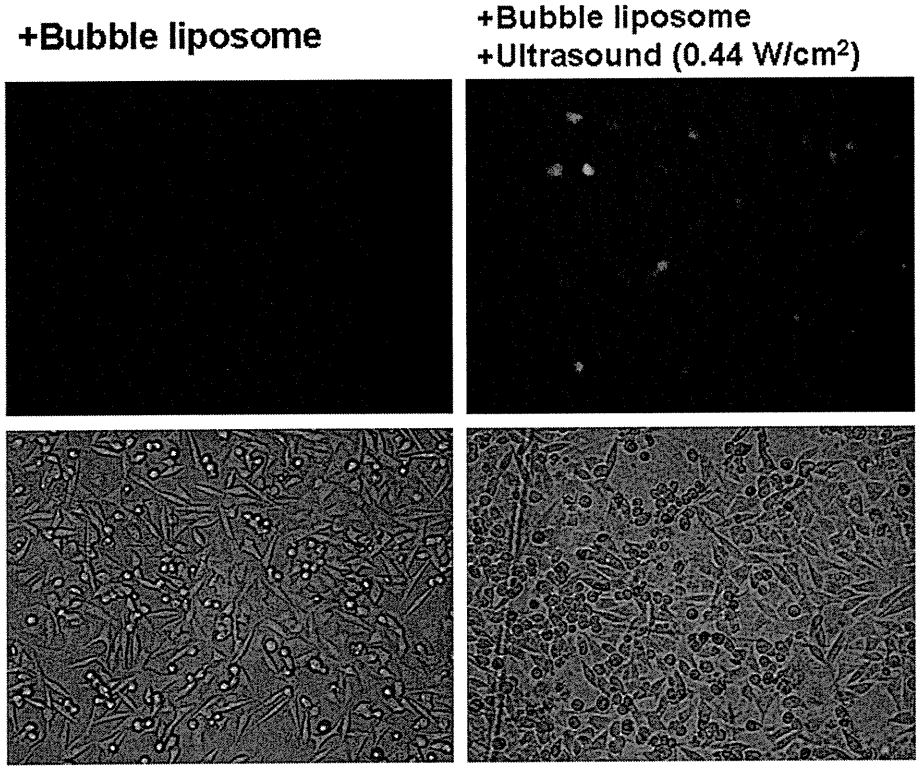

Fig. 6. Internalization of dextran–fluorescein conjugates by ultrasound irradiation with Bubble liposomes. Upper images show the detection of fluorescein into HeLa cells by fluorescence microscopy, and lower images show the condition of HeLa cells by light microscopy. After addition of dextran conjugates and Bubble liposomes on the cells, ultrasound was irradiated for 20 s or not.

hanced ultrasound to deliver antibiotic molecules into cells to eradicate intracellular bacteria without causing significant damage to the cells itself. This modality may become a new treatment modality for Chlamydial infection.

Acknowledgements

This work was supported in part by a Grant-in-Aid for Scientific Research on Priority Areas (18800075 and 20500432) from the Ministry of Education, Culture, Sports, Science and Technology, Japan and also in part by a grant from Fukuoka University Central Research Institute.

References

[1] R.W. Peeling, R.C. Brunham, Chlamydiae as pathogens: new species and new issues, Emerg. Infect. Dis. 2 (1996) 307–319.
[2] J. Schachter, Infection and disease epidemiology, American Society for Microbiology, Washington DC, 1999.
[3] W. Cates Jr., J.N. Wasserheit, Genital chlamydial infections: epidemiology and reproductive sequelae, Am. J. Obstet. Gynecol. 164 (1991) 1771–1781.
[4] K.A. Workowski, S.M. Berman, CDC sexually transmitted diseases treatment guidelines, Clin. Infect. Dis. 35 (2002) S135–137.
[5] D.H. Martin, T.F. Mroczkowski, Z.A. Dalu, J. McCarty, R.B. Jones, S.J. Hopkins, R.B. Johnson, A controlled trial of a single dose of azithromycin for the treatment of chlamydial urethritis and cervicitis. The Azithromycin for Chlamydial Infections Study Group, N. Engl. J. Med. 327 (1992) 921–925.
[6] A. Nilsen, A. Halsos, A. Johansen, E. Hansen, E. Torud, D. Moseng, G. Anestad, G. Storvold, A double blind study of single dose azithromycin and doxycycline in the treatment of chlamydial urethritis in males, Genitourin. Med. 68 (1992) 325–327.
[7] J.D. Oriel, G.L. Ridgway, Epidemiology of chlamydial infection of the human genital tract: evidence for the existence of latent infections, Eur. J. Clin. Microbiol. 1 (1982) 69–75.
[8] W.G. Pitt, M.O. McBride, J.K. Lunceford, R.J. Roper, R.D. Sagers, Ultrasonic enhancement of antibiotic action on gram-negative bacteria, Antimicrob. Agents Chemother. 38 (1994) 2577–2582.
[9] A.M. Rediske, B.L. Roeder, M.K. Brown, J.L. Nelson, R.L. Robison, D.O. Draper, G.B. Schaalje, R.A. Robison, W.G. Pitt, Ultrasonic enhancement of antibiotic action on *Escherichia coli* biofilms: an in vivo model, Antimicrob. Agents Chemother. 43 (1999) 1211–1214.
[10] A. Nagayama, T. Nakao, H. Taen, In vitro activities of ofloxacin and four other new quinoline-carboxylic acids against *Chlamydia trachomatis*, Antimicrob. Agents Chemother. 32 (1988) 1735–1737.
[11] R. Suzuki, T. Takizawa, Y. Negishi, K. Hagisawa, K. Tanaka, K. Sawamura, N. Utoguchi, T. Nishioka, K. Maruyama, Gene delivery by combination of novel liposomal bubbles with perfluoropropane and ultrasound [see comment], J. Control. Release 117 (2007) 130–136.
[12] T. Notomi, Y. Ikeda, A. Nagayama, Minimum inhibitory and minimal lethal concentration against *Chlamydia trachomatis* dependent on the time of addition and the duration of the presence of antibiotics, Chemotherapy 45 (1999) 242–248.
[13] K. Laasila, L. Laasonen, M. Leirisalo-Repo, Antibiotic treatment and long term prognosis of reactive arthritis, Ann. Rheum. Dis. 62 (2003) 655–658.
[14] T. Yli-Kerttula, R. Luukkainen, U. Yli-Kerttula, T. Mottonen, M. Hakola, M. Korpela, M. Sanila, J. Parviainen, J. Uksila, R. Vainionpaa, A. Toivanen, Effect of a three month course of ciprofloxacin on the outcome of reactive arthritis, Ann. Rheum. Dis. 59 (2000) 565–570.
[15] M.U. Rahman, M.A. Cheema, H.R. Schumacher, A.P. Hudson, Molecular evidence for the presence of chlamydia in the synovium of patients with Reiter's syndrome, Arthritis Rheumatism 35 (1992) 521–529.
[16] J.S. Gaston, Immunological basis of Chlamydia induced reactive arthritis, Sex. Transm. Infect. 76 (2000) 156–161.
[17] H. Hanada, Y. Ikeda-Dantsuji, M. Naito, A. Nagayama, Infection of human fibroblast-like synovial cells with *Chlamydia trachomatis* results in persistent infection and interleukin-6 production, Microb. Pathog. 34 (2003) 57–63.
[18] N. Reveneau, D.D. Crane, E. Fischer, H.D. Caldwell, Bactericidal activity of first-choice antibiotics against gamma interferon-induced persistent infection of human epithelial cells by *Chlamydia trachomatis*, Antimicrob. Agents Chemother. 49 (2005) 1787–1793.
[19] H.R. Guzman, A.J. McNamara, D.X. Nguyen, M.R. Prausnitz, Bioeffects caused by changes in acoustic cavitation bubble density and cell concentration: a unified explanation based on cell-to-bubble ratio and blast radius, Ultrasound Med. Biol. 29 (2003) 1211–1222.
[20] L.B. Feril Jr., T. Kondo, Q.L. Zhao, R. Ogawa, K. Tachibana, N. Kudo, S. Fujimoto, S. Nakamura, Enhancement of ultrasound-induced apoptosis and cell lysis by echo-contrast agents, Ultrasound Med. Biol. 29 (2003) 331–337.
[21] L.B. Feril Jr., R. Ogawa, K. Tachibana, T. Kondo, Optimized ultrasound-mediated gene transfection in cancer cells, Cancer Sci. 97 (2006) 1111–1114.

[22] M. Ward, J. Wu, J.F. Chiu, Experimental study of the effects of Optison concentration on sonoporation in vitro, Ultrasound Med. Biol. 26 (2000) 1169–1175.
[23] C.X. Deng, F. Sieling, H. Pan, J. Cui, Ultrasound-induced cell membrane porosity, Ultrasound Med. Biol. 30 (2004) 519–526.
[24] K. Tachibana, T. Uchida, K. Ogawa, N. Yamashita, K. Tamura, Induction of cell-membrane porosity by ultrasound, Lancet 353 (1999) 1409.
[25] L.B. Feril Jr., K. Tachibana, T. Kondo, R. Ogawa, Q.-L. Zhao, Y. Yamaguchi, K. Ogawa, H. Endo, Y. Irie, Y. Harada, Hypotonia-induced cell swelling enhances ultrasound-induced mechanical damage to cancer cells, J. Med. Ultrasonics 37 (2010) 3–8.

—Review—

超音波感受性リポソームを利用した超音波がん治療システムの開発

鈴木 亮,* 小田雄介, 宇都口直樹, 丸山一雄

Development of Ultrasonic Cancer Therapy Using Ultrasound Sensitive Liposome

Ryo SUZUKI,* Yusuke ODA, Naoki UTOGUCHI, and Kazuo MARUYAMA
Department of Biopharmaceutics, School of Pharmaceutical Sciences, Teikyo University, 1091-1 Suwarashi, Midori-ku, Sagamihara, Kanagawa 252-5195, Japan

(Received September 1, 2010)

Ultrasound (US) has been utilized as a useful tool for diagnosis and therapy. US mediated drug and gene delivery is paid to attention as a non-invasive system. The combination of US and microbubbles generated microjet stream by inducing disruption of bubbles and resulted in enhancing permeability of cell membrane. This phenomenon has been utilized as driving force for drug and gene delivery. Recently, we developed ultrasound sensitive liposome [Bubble liposome (BL)] containing perfluoropropane gas. US combined with BL could effectively transfer gene *in vivo* compared to conventional cationic liposomes. Using this method, we succeeded to obtain a therapeutic effect in cancer gene therapy with Interleukin-12 corded plasmid DNA. Therefore, it is expected that US combined with BL might be a useful non-viral vector system. From this result, the fusion of liposomal and ultrasound technologies would be important for establishment of advanced cancer therapy.

Key words——liposome; ultrasound; non-viral vector; drug delivery system (DDS); gene therapy

1. はじめに

リポソームは脂質二重膜からなる閉鎖小胞であり，その内部に薬物を封入したり，表面にポリマーや抗体などを修飾できる性質を有していることから，薬物キャリアーとして期待されている．実際に11品目のリポソーム製剤が世界中で上市されており，リポソーム技術は薬物治療の最適化を目指すドラッグデリバリーシステム（DDS）のための製剤技術として注目されている．その中で筆者らは，リポソームに関する研究を長年続けており，がん細胞にアクティブターゲティング可能な抗がん剤封入リポソームや中性子捕捉療法におけるがん組織へのボロン化合物送達システムとしてのリポソームの利用など様々なリポソーム開発に携わってきた.[1-3] そして最近では，新たな取り組みとしてリポソームの内水相部分に超音波造影ガスであるパーフルオロプロパンを封入した新たなタイプのリポソーム開発を行っている.[4-11] そこで本稿では，筆者らが開発を続けているリポソーム型微小気泡（バブルリポソーム）と超音波照射の併用によるがん遺伝子治療について紹介する．

2. バブルリポソームについて

近年の超音波技術の進展は目覚ましく，超音波造影装置の高解像度化や3D撮像などが可能となっている．そして最近では，超音波を数mm単位で患部に対し正確に照射することのできる強力集束超音波（High intensity focused ultrasound: HIFU）が開発され，超音波熱エネルギーによる前立腺がんや子宮筋腫の低侵襲的治療として医療の現場で利用され始めている．このように超音波技術は医療分野において診断及び治療に応用され，これからさらなる飛躍が期待されている．これに加え，超音波造影剤の開発も進められており，わが国においては世界に先駆け肝腫瘤性病変のための超音波造影剤であるSonazoidが上市された．このSonazoidは静脈内投与後，速やかに肝臓のクッパー細胞に取り込まれることで肝腫瘤病変を陰影像としてとらえることができる優れた超音波造影剤である．このように肝臓のクッパー細胞を利用した超音波造影が可能になるの

帝京大学薬学部生物薬剤学教室（〒252-5195 神奈川県相模原市緑区寸沢嵐 1091-1)
*e-mail: r-suzuki@pharm.teikyo-u.ac.jp
本総説は，日本薬学会第130年会シンポジウムS10で発表されたものを中心に記述したものである．

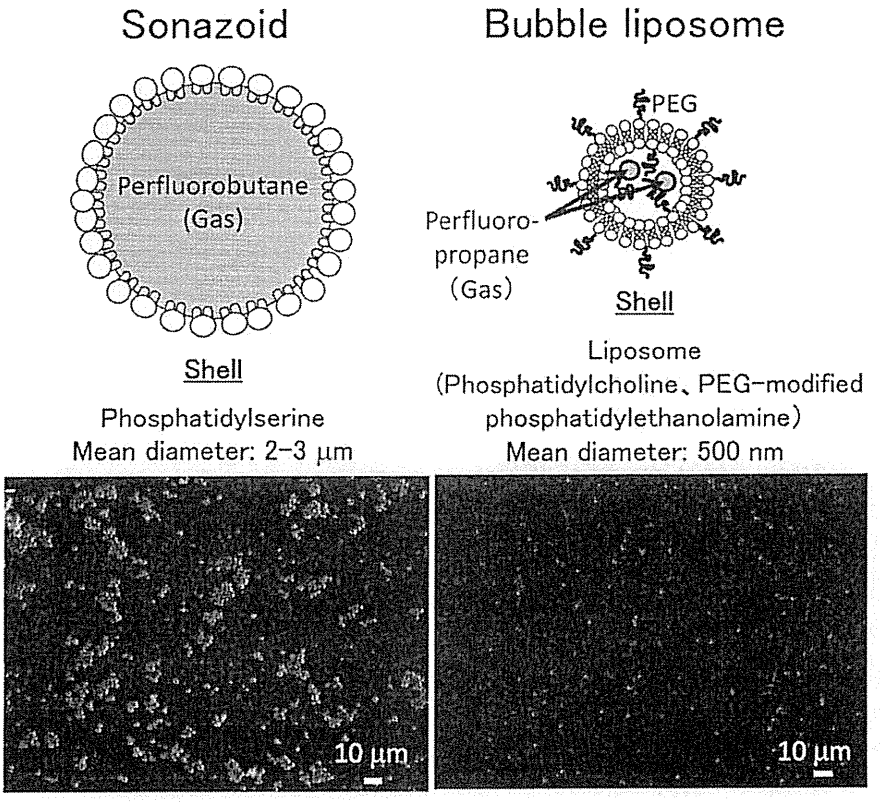

Fig. 1. Comparison of Sonazoid and Bubble Liposome
Scheme (upper) and microscope (×400) (lower)

は，Sonazoid がホスファチジルセリンからなる気泡であること，さらに粒子サイズが 2-3 μm でありクッパー細胞に積極的に貪食され易い性質を有しているためである．一方，われわれが開発したバブルリポソームは，粒子サイズが約 500 nm と Sonazoid より小さい上，ポリエチレングリコール（PEG）修飾リポソーム内に気泡が封入された構造であるため表面に存在する PEG の影響でクッパー細胞による貪食から逃れ易くなっている（Fig. 1）．したがって，粒子サイズ及びクッパー細胞などによる貪食の回避などの観点から，バブルリポソームが組織深部にまで到達可能になるものと期待される．

3. ソノポレーションを利用した遺伝子デリバリー

超音波を利用した遺伝子導入研究は 1987 年に Fechheimer らによる報告から始まった．[12] この超音波による遺伝子導入メカニズムとしてキャビテーション(空洞現象)が関与していると考えられている．キャビテーションとは，液体に超音波を照射したときの負の圧力が液体を維持するのに必要な圧力に打ち勝ったときに空洞を生じる現象である．このキャビテーション気泡は最終的に圧壊するが，この圧壊時に気泡近傍にジェット流が生じ，このエネルギーにより細胞膜に一過性の小孔が開くことで，細胞外の物質が細胞内に送達されると考えられている．しかし，超音波を利用した初期の遺伝子導入ではキャビテーションの誘導効率を高めるために 20-50 kHz の低い周波数の超音波が用いられており，細胞に対する傷害性が問題となっていた．これは低い周波数ほど低い強度でキャビテーションを誘導可能であるが，キャビテーション気泡の直径が大きくなり細胞に対する傷害性が高くなってしまったと考えられた．一方，高い周波数の超音波ではキャビテーショ

鈴木 亮

帝京大学薬学部生物薬剤学教室講師．博士（薬学）．1973 年神奈川生まれ．東京薬科大学卒業，大阪大学大学院薬学研究科博士課程修了．2001 年東レ株式会社入社，2004 年帝京大学薬学部助手，2007 年同助教，2010 年現職．リポソーム技術を駆使した革新的がん治療システムの構築に関する研究に従事．